Synthesis and Characterization of a New Perylene Anhydride Derivative Functionalized at the Bay Region

Brhan Ramadhan Al-Zebari

Submitted to the
Institute of Graduate Studies and Research
in partial fulfillment of the requirements for the Degree of

Master of Science
in
Chemistry

Eastern Mediterranean University
June 2014
Gazimağusa, North Cyprus

Approval of the Institute of Graduate Studies and Research

<div style="text-align: right">

_____
Prof. Dr. Elvan Yılmaz
Director
</div>

I certify that this thesis satisfies the requirements as a thesis for the degree of Master of Science in Chemistry.

<div style="text-align: right">

_____
Prof. Dr. Mustafa Halilsoy
Chair, Department of Chemistry
</div>

We certify that we have read this thesis and that in our opinion it is fully adequate in scope and quality as a thesis for the degree of Master of Science in Chemistry.

<div style="text-align: right">

_____
Prof. Dr. Huriye İcil
Supervisor
</div>

Examining Committee
_____

1. Prof. Dr. Huriye İcil   _____

2. Asst. Prof. Dr. Nur P. Aydınlık   _____

3. Asst. Prof. Dr. Mustafa E. Özser   _____

ABSTRACT

Perylene chromophore has an outstanding aromatic conjugation. The functionalization at the bay and imide positions brings great advantages. Specifically, functionalization at the bay region via long alkyl chain improves the solubility as well as the optical and electrochemical properties.

In this thesis study, we have synthesized a new bay-substituted perylene dianhydride, (1,7-di(2-decyl-1-tetradecanoyl)-perylene-3,4,9,10-tetracarboxylic dianhydride; decanol-PDA) in two steps. In the first step, the bay positions (1, 7-positions) of perylene dianhydride (PDA) were brominated (Br-PDA). In the second step, the targeted bay substituted perylene dianhydride (decanol-PDA) was synthesized through bay substitution of perylene core with 2-decyl-1-tetradecanol.

The product was purified and characterized by using FTIR spectroscopy, UV-vis spectroscopy and emission spectroscopy. Expectively, the synthesized product showed enhanced solubility comparing perylene anhydride.

The UV-vis absorption spectra of the two synthesized perylene derivatives in nonpolar solvents showed three characteristic absorption bands, that are belonging to π–π* electronic transitions of perylene chromophore. While, the UV-vis absorption spectra in dipolar aprotic solvents showed additional absorption bands at higher wavelength. The emission spectra of the synthesized compounds showed excimer-like emission spectra in nonpolar and dipolar aprotic solvent.

Keywords: Perylene dianhydride, bay-substitution, optical and photophysical properties.

ÖZ

Perilen kromoforu zengin aromatik yapıdadır. Gerek körfez gerekse imid bölgesinde fonksiyonlaştırma sayesinde çok farklı fotonik özelliklere ulaşılabilmesi avantaj teşkil etmektedir. Körfez bölgesinde özellikle uzun ve dallanmış yapıda alkiller ile fonksiyonlaştırma çözünürlük yanında optik ve elektrokimyasal özellikleri değiştirilebilmektedir.

Bu çalışmada 1,7-di(2-desil-1-tetradekanoil)-perilen-3,4,9,10-tetrakarboksilik dianhidrit (Decanol-PDA) iki aşamada sentezlenmiştir. İlk aşamada körfez bölgesinde bromlanma gerçekleştirilerek (1,7-pozisyonları) bromlanmış perilen dianhidrit elde edilmiştir (Br-PDA). İkinci aşamada ise hedeflenen körfez sübstitüe ürün 2-desil-1-tetradekanol kullanımıyle substitasyon reaksiyonu ile sentezlenmiştir.

Ürün saflandırılarak FTIR, UV-vis ve emisyon spekroskopi yöntemleri kullanılarak karakterize edilmiştir. Bekendiği gibi ürünün organik çözgenlerdeki çözünürlüğü perilen dianhidrite gore oldukça yüksektir.

Sentezlenen iki ürünün apolar çözgenlerde alınan UV-vis absorpsiyon spektrumlarında $\pi–\pi*$ elektronik geçişlerini gösteren karakteristik üç band elde edilmiştir. Halbuki dipolar aprotik çözücülerde uzun dalga boylarında ek bandlar gözlenmiştir. Ürünler gerek apolar gerekse dipolar aprotik çözücülerde ekzimer emisyonu vermektedir.

Keywords: Perilen dianhidrit, körfez substitasyon, optik ve fotofiziksel özellikler

To My Family

ACKNOWLEDGMENT

First of all, I am really thankful to my supervisor Prof. Dr. Huriye İcil for all her orientation, encouragement and support during my work in master thesis and also for her advices in general life.

Also, I would like to thanks Dr. Duygu Uzun which helped me a lot during my thesis work.

Likewise, I am grateful to my dear father for his constant support, encouragement and advice throughout my life and his words of inspiration and encouragement in pursuit of excellence, still linger on.

I would like to sincerely thank my mother who taught me the meaning of love and compassion and whose du'aa was the secret behind my success.

Finally, I am thankful to my brothers, sisters, wife, son, daughter, all my relatives, teachers and friends.

TABLE OF CONTENTS

LIST OF TABLES

LIST OF FIGURES

LIST OF SCHEMES

LIST OF SYMBOLS/ABBREVIATION

$\overset{\circ}{\text{A}}$	Armstrong
A	Absorption
AU	Arbitrary Unit
CHL	Chloroform
c	Concentration
cm	Centimeter
E_g	Band gap energy
ºC	Degrees celcius
$\Delta\bar{\nu}_{1/2}$	Half-width of the selected absorption
ε_{max}	Maximum extinction coefficient
f	Oscillator strength
λ_{max}	Absorption wavelength maximum
λ	Wavelength
τ_0	Theoretical radiative lifetime
τ_f	Fluorescence lifetime
Φ_f	Fluorescence quantum yield
nm	Nanometer
DMF	N,N`-dimethylformamide
DMSO	N,N`-dimethyl sulfoxide
MeOH	Methanol
FTIR	Fourier Transform Infrared Spectroscopy
KBr	Potassium bromide

M	Molar concentration
UV-vis	Ultraviolet visible absorption spectroscopy
OLED	Organic light emitting diode
PDI	Perylene diimide
PDA	Perylene dianhydride
OFET	Organic field-effect transistor
HOMO	Highest occupied molecular orbital
LUMO	Lowest unoccupied molecular orbital
SC	Solar cell
OSC	Organic solar cell
ITO	Indium tin oxide
h	Hour
l	Path length
$\bar{\nu}$	Wavenumber
$\bar{\nu}_{max}$	Maximum wavenumber/Mean frequency
E_s	Singlet energy
Br-PDA	1,7-dibromoperylene-3,4,9,10-tetracarboxylic dianhydride
Decanol-PDA	1,7-di(2-decyl-1-tetradecanoyl)-perylene-3,4,9,10-tetracarboxylic dianhydride
s	Second
g	Gram
TLC	Thin layer chromatography
Br_2	Bromine
d	Density
k_f	Fluorescence rate constant

Chapter 1

INTRODUCTION

Perylene-3,4,9,10-tetracarboxylic diimide (PDI) shortly perylene dye was firstly revealed in 1913 by Kardos [1]. Perylene-3,4,9,10-tetracarboxylic dianhydride (PDA), which is generally considered as the origin compound of this type of dyes, was described for the first time in 1912. Figure 1.1 shows the general structure of PDA and PDI. As shown in the Figure 1.1, different perylene dyes can be obtained with various physical and chemical properties via substitution at the bay (1, 6, 7, and 12) positions and imide positions [2-6].
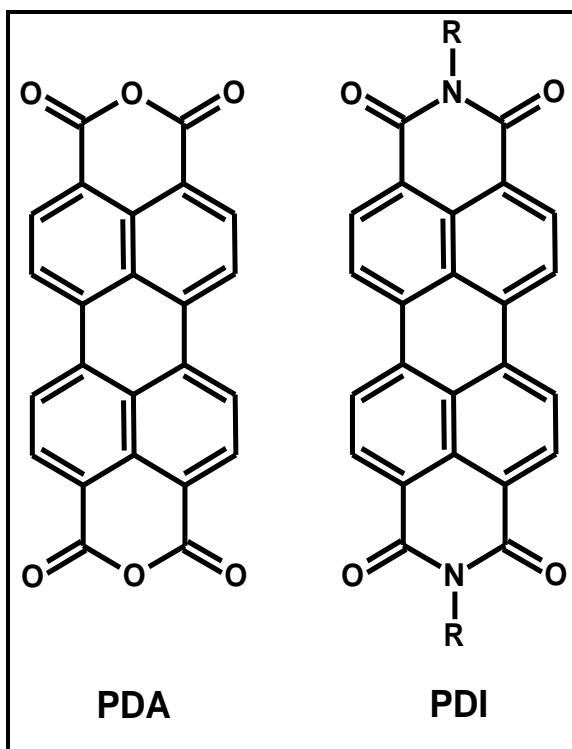
Figure 1.1: A General Structure of PDA and PDI

Perylene diimides (PDIs) have attracted significant care in educational research as well as pigment and industrial dyes, due to their good thermal and photochemical stabilities, excellent photoluminescence, highly fluorescence quantum yields, the best n-type organic semiconductors, solid electron acceptors, rapid electron transferring properties, and show great optical absorption in the visible region [1-13]. These properties make them suitable in various applications, such as, organic solar cells, electronic resources, dye lasers, sensors, and organic field-effect transistors (OFETs) [1-3, 8-11, 14].

Unfortunately, PDIs have poor solubility in most of the organic solvents, because of the strong PDI π-π stacking interactions, however, researchers founds various ways to increase the solubility of perylene diimide including: substituting bulky substituent into the bay positions of perylene core, connecting long alkyl elastic groups into the imide positions, and copolymerization of PDI together with additional monomer [1, 4, 6, 7, 14-23].

The aim of this project is to synthesize a new perylene dianhydride derivative functionalized at the bay region, namely 1,7-di(2-decyl-1-tetradecanoyl)-perylene-3,4,9,10-tetracarboxylic dianhydride (Decanol-PDA). The synthesis carried out in two steps. Firstly, the perylene dianhidride (PDA) brominated in core positions to form 1,7-dibromoperylene-3,4,9,10-tetracarboxylic dianhydride (Br-PDA). Secondly, the Br-PDA was reacted with 2-decyl-1-tetradecanol to produce 1,7-di(2-decyl-1-tetradecanoyl)-perylene-3,4,9,10-tetracarboxylic dianhydride (Decanol-PDA). The synthesized products followed by detailed characterization to discover well their optoelectronic properties, using UV-vis and emission spectra. Structural characterization was performed by FTIR.

2
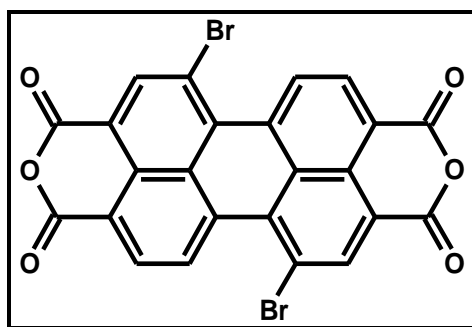
Figure 1.2: The Structure of Br-PDA
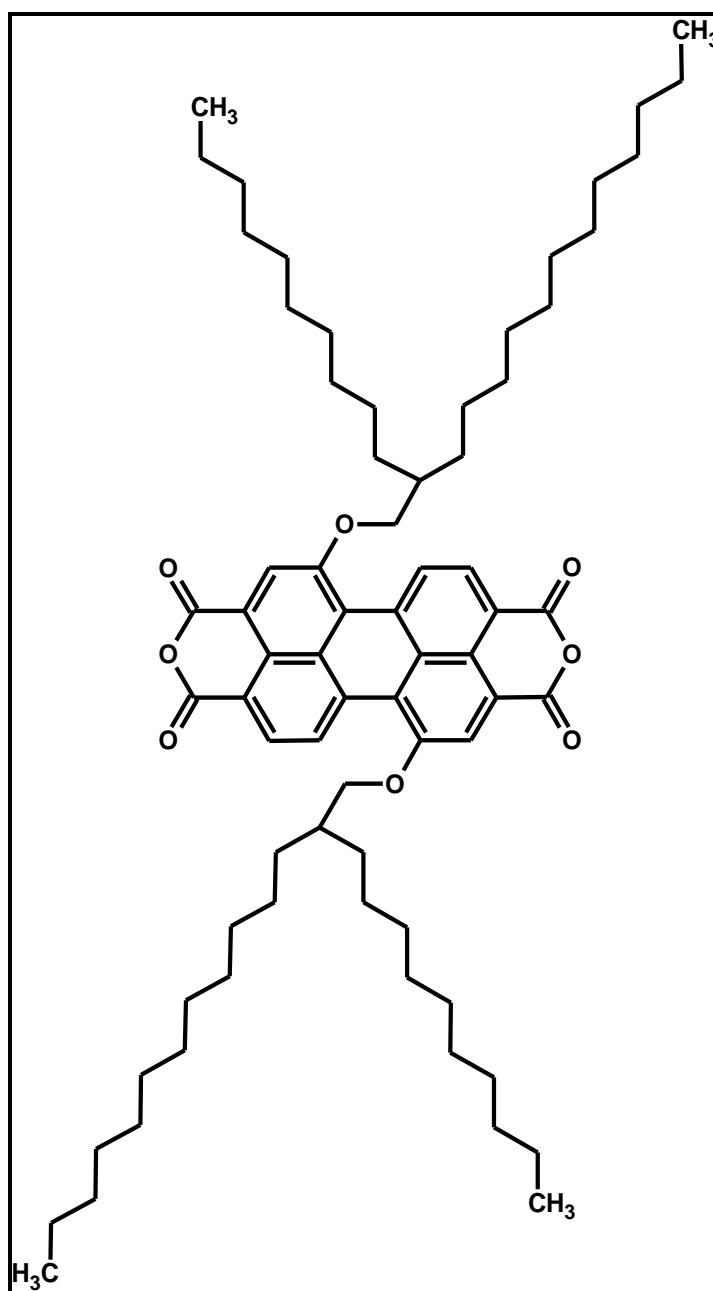
Figure 1.3: The Structure of Decanol-PDA

Chapter 2

THEORETICAL

2.1 Perylene Dyes: Promising Organic Materials

One of the most widely studied organic semiconductors is the derivatives of PDI, due to their strong electron accepting properties, extremely light fastness and high fluorescence quantum yields. The ability of the PDI to absorb and convert sunlight to electrical power made them applicable in organic photovoltaic cells [2, 6, 14, 23, 24].

2.1.1 Structural Properties of Perylene Dyes

The major feature of PDI is their structure that has the possibility to modulate easily by introducing different substituent groups at the imide nitrogen and at bay positions. Then, the physical, optical and electronic properties of the materials obtained changed according to the types of substituents. [2, 4-6, 12, 14, 24].

The carbonyl groups present in the structure of PDI bring the electron accepting properties and thus acts as significant electron acceptor. One of the best n-type semiconductors is the derivatives of PDI. Therefore they are promising for organic electronic applications, like solar cells (SCs) and OFETs due to their high electron affinity [14, 25].

Also, the PDI molecules can be inserted into the structure of polymers to improve the solubility and the processability. Generally, there are two ways to integrate PDI units into polymer series. First one is to introduce PDI units into the polymer backbone to

act as electron acceptor units in OFETs and SCs. Another one is to rope PDI units along a polymer backbone as pendants [24].

2.1.2 Core and Imide Substitution of Perylene Chromophore

PDI is well known as a chemically versatile building block. The chemical modulation of their structure can be easily achieved. Also their properties, like highest occupied molecular orbital (HOMO) and lowest unoccupied molecular orbital (LUMO) energy levels, can be simply and specifically tailored by introducing different chemical substituent groups at the imide nitrogen positions or bay positions (Figure 2.1) [4, 14].
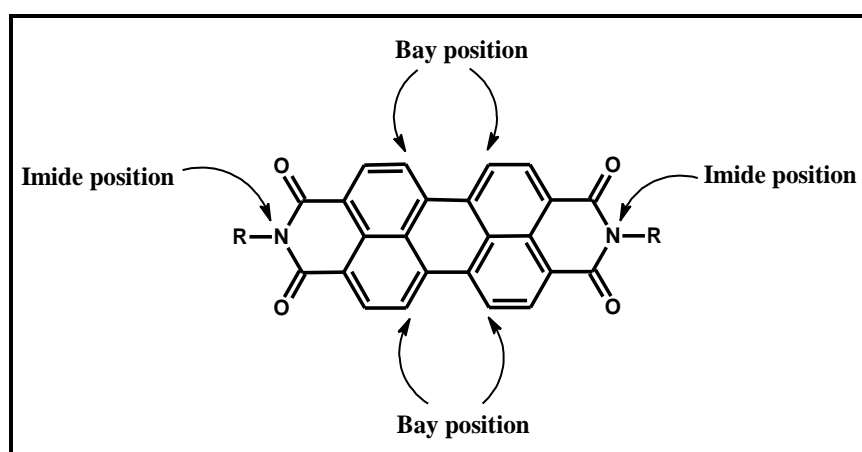
Figure 2.1: Core and Imide Positions of Perylene Diimide

The substitution at the bay position has an obvious influence on the absorption and emission properties of the PDIs, due to the strong electronic coupling between the substituents at the bay positions and the PDI's π-orbitals [14].

The core-functionalization of PDI at 1, 6, 7, and 12 positions, depending on the conformation and therefore the kind of the substituent groups, results a structural and an electronic influence on the perylene diimide chromophore. Substituent groups that have high steric hindrance connected at bay position hamper the π-π stacking and

aggregation of PDI and decrease the charge mobility growing together the solubility. When a heteroaromatic or aromatic group that is electron-reach donor is covalently connected to perylene core, the Donor-Acceptor system is formed via a charge transfer between the PDI moieties and the donor, and therefore, the energy gap is reduced [14].

On the other hand, introducing different organic substituent groups at the imide nitrogen affects the properties of perylene diimides in the solid state and their solubilities. However it has less impacts in the emission and the absorption properties, because of the nodes in the HOMO and LUMO at the N atom that decrease the coupling between the imide substituents and the perylene core [14, 22].

Commonly, the imide positions of the perylene dyes are replaced by alkyl chains, usually branched, so as to obtain good solubility of the compound [4, 21]. It is known that, the products of perylene via symmetrical and asymmetrical alkyl groups at the nitrogen positions without core substituents have very high thermal stability with extraordinary decay temperatures [4].

Finally, attaching organic substituent groups at the N-position is usually used to improve the solubility, whereas the introduction of substituent at the core position likewise affects the electrochemical and optical properties and adjust the energy levels [14]. However, when maintaining planarity of the perylene core is substantial, the imide positions are the favored places to introduce solubilizing groups [6].

2.2 Characterization of Perylene Dyes

The conjugated compounds that act as *n*- and *p*- type materials want to be fine characterized, so as to discover their possibility to utilize in applications. The optical and electronic properties show an important character to find the stability of the compounds and thus their usage in various applications [26].

2.2.1 Optical Properties

Perylene diimides show a promising redox, absorption and emission properties. Most of the perylene diimides are red solids and have high thermal- and photo-stabilities with high melting points. Also, perylene diimides with different colors are known, such as, bluish black, maroon, orange, and black [27].

Generally, perylene diimides have large molar absorptivities at the visible region of the absorption spectrum (wavelengths 400‑550 nm), long life-times of singlet excited state (around 4ns in common organic solvents), show strong fluorescence and fluorescence quantum yields are near unity (the fluorescence spectrum and absorption spectrum are nearly mirror image of each other, and shows a small Stokes shift) [12, 15].

Furthermore, optical properties of PDIs are greatly dependent on the temperature, solvent polarity, and concentration. For instance, at high concentration solutions, aggregation between the aromatic scaffolds give rise to broader absorption range and great bathochromic shift, with absorption that extends into the near infrared [15].

2.2.2 Electronic Properties

Electronic properties of *n-* and *p-* type substances, like, oxidation-reduction potentials, HOMOs, LUMOs and energy band gaps, create a complete band structure of the compound and therefore help finding the suitable electron donor, corresponding to a donor-acceptor system for photovoltaic devices [26].

PDIs have characteristically high electron affinity, and as a result, they are good electron acceptors. They are reducing easily and relatively oxidized harder [2, 25]. Like optical properties, the type of the imide substituents has a very small influence on the oxidation-reduction potentials. Conversely, the bay-substituents have substantial impact on the oxidation-reduction characteristics of the perylene diimides [14].

Introducing strong electron withdrawing substituent groups at the bay positions of PDIs, makes PDIs reduced more easily [14]. Moreover, introducing conjugated substituents at the bay regions of PDI have mostly increased the ability of PDI derivatives to reduce. This is possibly due to the extent of π-conjugation [2].

In addition, existence of electron donating groups at the bay-positions reduces the electronaccepting capability of PDIs, because it makes the PDIs electron rich. Also, it has the main effect on the band gap and the HOMO and LUMO orbital energy levels of the resultant perylene diimide compound [14, 28].

2.3 An Overview on Solar Cells

The device that produces electrical energy from solar energy by photovoltaic effect is called a solar cell. The expression solar cell is used for devices that precisely take energy from sunshine, but when the source of energy/light is unknown the expression photovoltaic cell, is used [26].

The replacing of the fossil fuel by renewable energy sources, for instance, solar cell, is one of the largest challenges ahead of human kind, because the conventional energy sources are consuming quickly and the population is growing rapidly. Furthermore, the bad influence of the traditional energy on the environment obliges to resort to alternative energy. Substantial use of traditional energy affects the balance of nature, the enormous quantities of carbon dioxide (CO_2) created in the air cannot be absorbed by the plants, and therefore, caused the global warming. An apparent source of inexpensive and pure energy is the Sun [26, 29].

It was quickly understood that such solar cells (SCs) were a suitable method of producing power in distant places. For instance, for running weather watching stations or communications apparatus, and perfect for giving power for vehicles being advanced for the speedily expanding universe manufacturing. Also the technology has nowadays been organized for an extensive variety of implementations, e.g. garden lights, electronic calculators, street lighting and water pumping [30].

Until now, available solar cells consist of inorganic semiconductors, which their fabrication needs great energy and thus high costs. Besides that, the most of those substances will consumed in near future and are poisonous [29].

Organic solar cells (OSCs) are more attractive than the classical inorganic solar cells due to the low cost and flexibility of the organic compounds [14, 29, 31]. In OSCs, the formation of electricity from sunlight is based on the process of photoinduced electron transfer containing two semiconducting substances, one electron-acceptor and one electron-donor, with different electron affinity and ionization potential [4, 14].

The primarily generation of OSCs was based on single organic layers inserted between two metallic electrodes. The following innovation was attained by inserting the bilayer heterojunction concept. In this method double organic layers with specific hole or electron transporting properties were sandwiched between the electrodes [32]. Recent development for OSC from the perspective of increasing the conversion efficiency is mainly attributed to the bulk heterojunction structure that widely allows an efficient charge separation, because the photo active boundary area of *p-n* junction is increased (Figure 2.3). The bulk *p-n* heterojunction is achieved generally by mixing a *n*-type conjugated polymer and a *p*-type conjugated polymer [33].
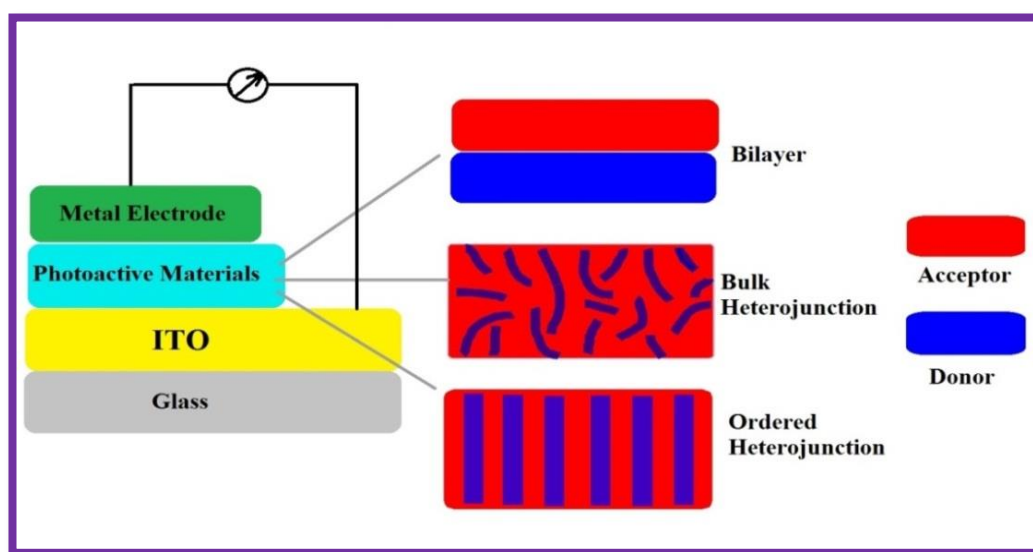
Figure 2.2: Graphic Diagram of a Various Organic Solar Cell Devices

2.4 Potential Applications of Perylene Diimide-Based Materials

Substituted PDIs are photochemically and thermally stable semiconductors. They have been incorporated in optical and electronic devices such as photovoltaic devices, electrophotographic applications, and field-effect transistors. Moreover, their light emitting capacity makes them applicable in organic light emitting diodes (OLEDs) and laser dyes [34].

2.4.1 Perylene Polymeric Materials in the Field of Organic Electronics

During the recent years, a remarkable advance in the domain of organic electronics has been made [35]. Organic electronics, including organic capacitors, organic thin film transistors, OLEDs, OFETs, organic material based sensors, and printable circuits were totally built on organic semiconductors. Most of these semiconductors are organic compounds that are polymer or high conjugated molecules that permit the movement of charge carriers [14, 26, 36, 37].

Perylene polymers are one of the organic semiconductors that offer numerous benefits, for instance, very high elasticity, low fabrication cost, and light weight. Moreover, conjugated polymers have simple processing and have the ability to modify electronic characteristics. Because of those properties, it's used in a variety of organic electronics [14, 37, 38].

Organic Light-Emitting Diodes (OLEDs)

In 1987 Tang and VanSlyke described the first thin-film (OLEDs) devices, which built on semiconductor films inserted among two electrodes, and the first polymer OLED was defined by Friend and et al. in 1990. OLEDs are classically made-up on glass covered with conducting indium tin oxide (ITO), and generally manufactured by vacuum thermal streaming of the organic layers on the (ITO) covered substrate.

Where the anode electrode is the ITO and the cathode is aluminium metal, the organic layers always contain the hole transport layers, emitting layer, and an electron transport layer (Figure 2.4) [39].
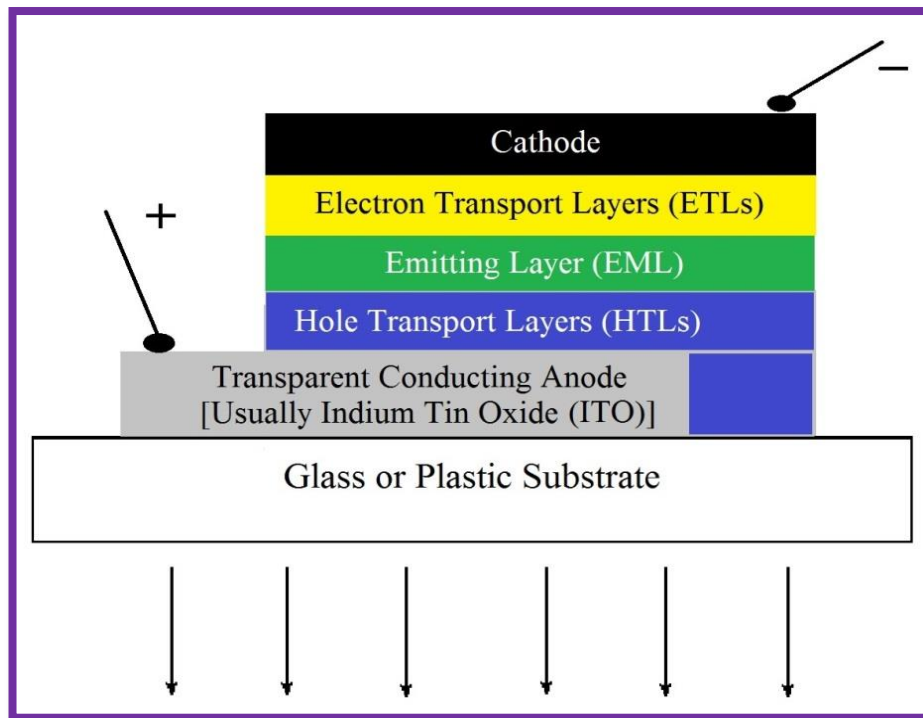
Figure 2.3: The Basic Structure of a Typical OLED

One of the developing exhibition technologies is OLED, particularly for handheld movable displays [28]. Owing to the unusual optical and electrical properties of conjugated polymers, it has concerned a lot of interest in polymer light emitting diodes [16]. Ego et al. industrialized numerous light emitting diodes based on the copolymers organized by connecting perylene dye to the side chains or termini chain of the polyfluorene [40].

Organic Field-Effect Transistors (OFETs)

Due to the next generation electronics, a numerous field effect transistor devices have been manufactured with thin films of molecular organics. Usually, the OFETs compared to the traditional field effect transistors with inorganic materials have low values of field effect movement. Nevertheless, they have numerous benefits, for example, structural elasticity, shock resistance, its covering large-area, and low price manufacturing, in contrast with conventional field-effect transistors [41].

The modern approaches to recent organic materials for field effect transistor devices, fundamentally, depend on the employment of pentacene and another conjugated organic acene for instance, tetracene [41].

Perylene dyes represent a hopeful family of materials amongst the large number of poly conjugated systems, that their characteristics, such as, luminescent, electronic, and electrochemical can be exploited in different kinds of devices, between them in OFETs. The modification of those characteristics can be achieved by inserting suitable functional group like electron accepting moieties, and then lead to air stability of n-channel OFETs [28].

Chapter 3

EXPERIMENTAL

3.1 Materials

Perylene-3,4,9,10-tetracarboxylic dianhydride, dimethyl formamide, 2-decyl-1-tetradecanol, dimethyl sulphoxide, bromine, iodine, and acetic acid were obtained from SIGMA ALDRICH. While potassium carbonate was obtained from MERCK.

Solvents like chloroform and methanol were purified by distillation, whereas, spectroscopic solvents directly used for spectroscopic analysis without additional purification.

3.2 Equipments

FTIR spectra

Infrared spectra of the compounds were recorded with a JASCO FT-IR-6200 by using potassium bromide pellets.

UV-vis spectra

Varian Carry-100 UV-visible spectrophotometer was used to measure absorption (UV-vis) spectra of the compounds in different solvents.

Emission spectra

Varian Cary Eclipse spectrophotometer was used to measure fluorescence quantum yield and emission spectra in different solvents.

3.3 Synthetic Methods of the Designed Perylene Anhydride Derivative Functionalized at the Bay Region

The purpose of this research is to synthesize a new bay substituted perylene dianhydride which is 1,7-di(2-decyl-1-tetradecanoyl)-perylene-3,4,9,10-tetracarboxylic dianhydride (Decanol-PDA). This synthesis was attained by two steps.

In the first step, the starting material perylene-3,4,9,10-tetracarboxylic dianhydride (PDA) was converted to 1,7-dibromoperylene-3,4,9,10-tetracarboxylic dianhydride (Br-PDA) (Scheme 3.1).

In the second step, the synthesized Br-PDA was converted to 1,7-di(2-decyl-1-tetradecanoyl)-perylene-3,4,9,10-tetracarboxylic dianhydride (Decanol-PDA) (Scheme 3.2).
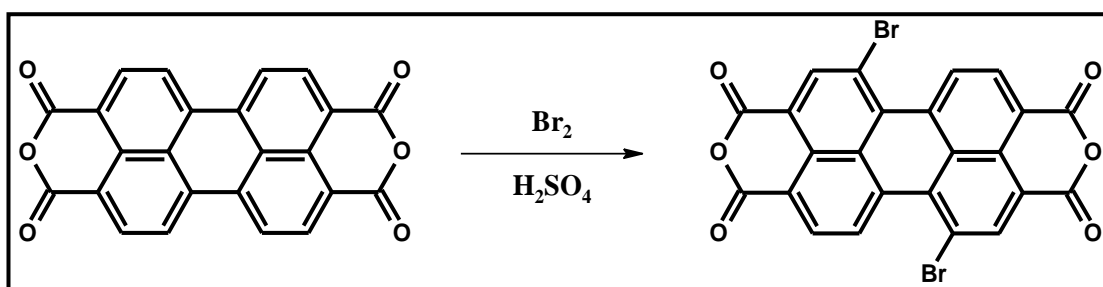
Scheme 3.1: Synthesis of Br-PDA
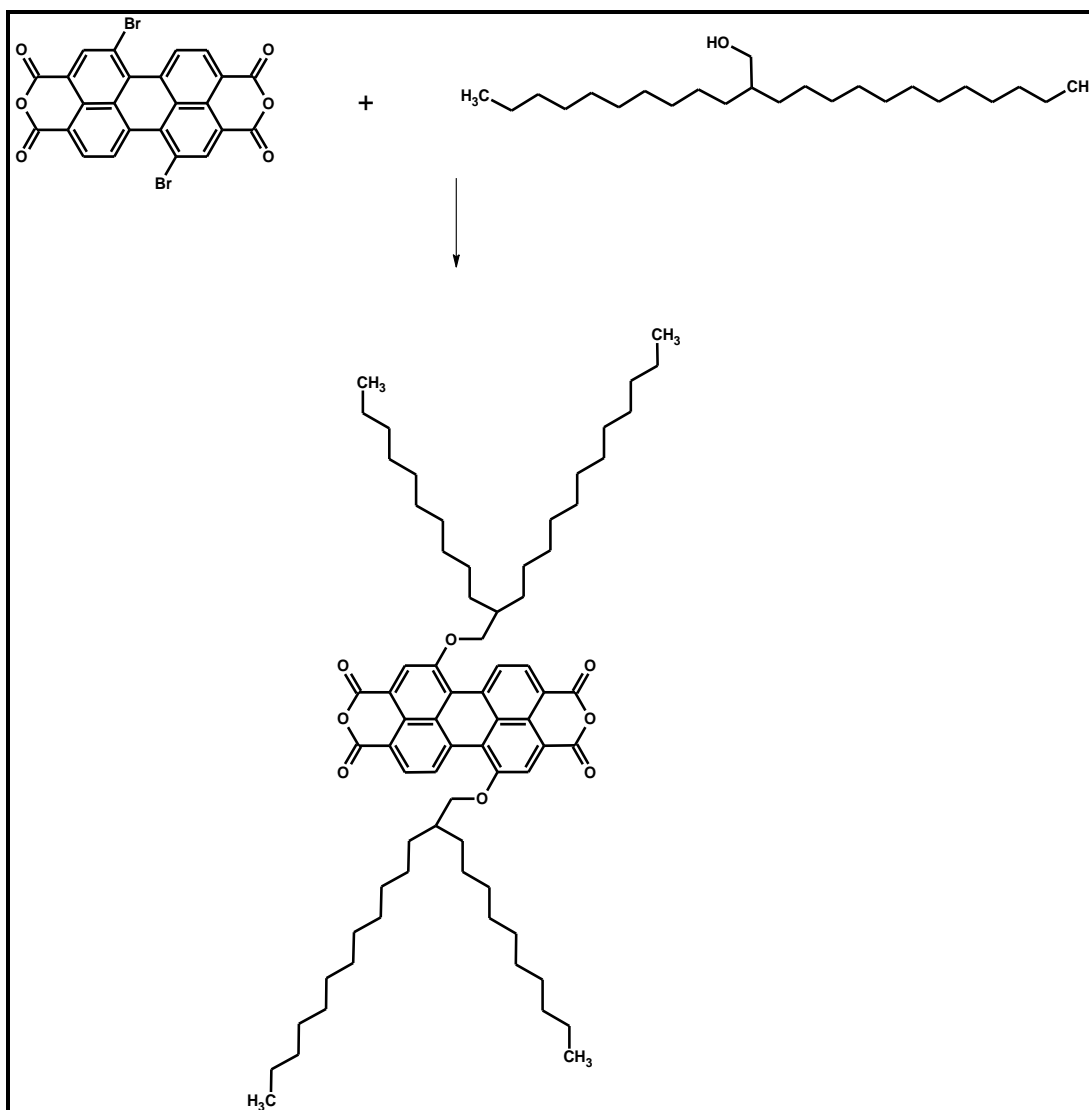
Scheme 3.2: Synthesis of Decanol-PDA

3.3.1 Synthesis of Brominated Perylene Bisanhydride (Br-PDA)
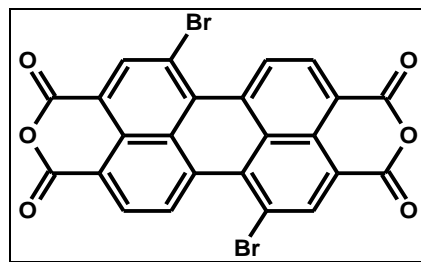
A mixture of perylene-3,4,9,10-tetracarboxylic dianhydride (3.9252 g, 10.00 mmol), sulfuric acid (32 ml, 95-97%, d = 1.84 g/cm^3), and iodine (I$_2$) (0.0963 g, 0.375 mmol) was refluxed for 1 hour at 35 ℃, 1 hour at 45 ℃, and 16 hours at 55 ℃. Then bromine (1.13 ml, 22 mmol, d = 3.119 g/cm^3) was added dropwise during a time period of two hours at room temperature. The mixture was stirred 48 hours at room temperature (isopropanol condenser at 5 ℃ was used), and then heated at 40 ℃ for 24 hours and at 85 ℃ for 6 hours, subsequently cooled to room temperature. In order to remove the excess bromine, a gentle stream of argon gas was passed through the reaction mixture. The reaction mixture was poured into a beaker contain of 250 ml of water, and kept in the fridge to overnight. The mixture was filtered off by a suction filtration. Then the precipitate was washed with a mixture of 250 ml water and 37.5 ml 86% sulfuric acid and kept overnight in the fridge. Finally, the precipitate was purified by water soxhlet for 24 hours and dried in a vacuum oven.

Yield: 90 %**, Color:** Light red

FT-IR (KBr, cm^{-1}): ν = 3058, 1770, 1723, 1591, 1036, 692.

UV-Vis (CHL) (λ_{max}/nm; (ε_{max}/L.mol^{-1}.cm^{-1})): 455 (30000), 487 (71500), 520 (99000).

Emission (CHL) (λ_{max}/nm): 552, 579; **Φ_f** = 0.57

R_f = 0 (Eluent: CHL, Acetone, Formic acid (10: 2: 2))

3.3.2 Synthesis of 1,7-di(2-Decyl-1-tetradecanoyl)-perylene-3,4,9,10-tetracarboxylic Dianhydride (Decanol-PDA)
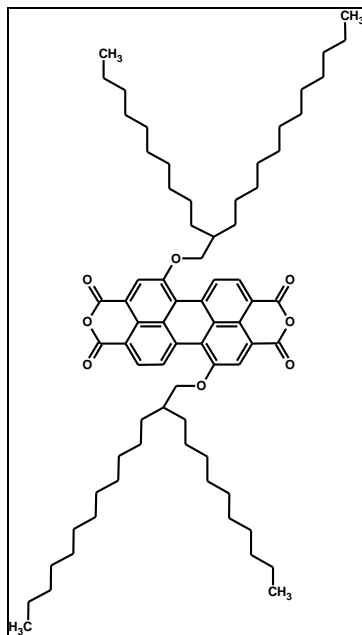
A mixture of Br-PDA (1.018 g, 1.85 mmol), 2-decyl-1-tetradecanol (1.56 ml, 3.70 mmol) and K_2CO_3 (0.257 g, 1.85 mmol) were refluxed for 32.5 hours in 150 ml DMF under argon atmosphere. Then the reaction mixture was poured into 140 ml of cold acetic acid and water (40 : 100 v/v) mixture and cooled to -8 °C overnight. The product was filtered off by suction filtration, and the obtained crude product was purified by water soxhlet for 24 hours, and then dried in a vacuum oven for 16 hours at 110 °C.

Yield: 85 %**, Color:** Black solid**.**

FT-IR (KBr, cm^{-1}): ν = 3129, 2924, 2853, 1765, 1734, 1593, 1466, 1018.

UV-vis (CHL) (λ_{max}/nm; (ε_{max}/L.mol^{-1}.cm^{-1})): 480 (20300), 515 (27600), 547 (28500).

Emission (CHL) (λ_{max}/nm): 533, 574; Φ_f = 0.30

R_f = 0 (Eluent: CHL, Acetone, Formic acid (10: 2: 2))

Chapter 4

DATA AND CALCULATION

4.1 Calculation of Fluorescence Quantum Yield (Φ_f)

The fluorescence quantum yield is defined as the ratio of the number of photons emitted to the number of photons absorbed by fluorescence and expressed as:

$$\Phi_f = \frac{\text{number of photons emitted}}{\text{number of photons absorbed}}$$

Fluorescence quantum yield is an important factor to specify the properties of a molecule, if all the absorbed light are emits by molecules or the absorbed light are deactivated by heat. The maximum fluorescence quantum yield is 1.0 (100%). High quantum yields are necessary for the application of photochemical reactions in organic syntheses. The comparative method of Williams et al. is the most dependable method for calculating Φ_f of a compound, this method uses well characterized standard samples that its Φ_f is known. It is considered that, both standard and test compounds solutions have absorbed equal number of photons at the same excitation wavelength. The quantum yield values are obtained by the ratio of integrated fluorescence intensities of the two solutions. The Φ_f value of unknown compound is calculated by using the following equation and a standard compound that its Φ_f is known.

$$\Phi_f(U) = \frac{A_{std}}{A_u} \times \frac{S_u}{S_{std}} \times \left[\frac{n_u}{n_{std}}\right]^2 \times \Phi_{std}$$

Φ_f (U) : Fluorescence quantum yield of unknown

A_{std} : Absorbance of the reference at the excitation wavelength

A_u : Absorbance of the unknown at the excitation wavelength

S_{std} : The integrated emission area across the band of reference

S_u : The integrated emission area across the band of unknown

n_{std} : Refractive index of reference solvent

n_u : Refractive index of unknown solvent

Φ_{std} : Fluorescence quantum yield of reference [42].

The fluorescence quantum yields of the synthesized perylene dyes calculated by using the N,N′-bis(dodecyl)-3,4,9,10-perylenebis(dicarboximide) as reference compound ($\Phi_f = 1$) [17]. All the perylene dyes including the reference were excited at $\lambda_{exc} = 485$ nm.

The Φ_f calculation of Decanol-PDA in CHL

The reference is N,N′-bis(dodecyl)-3,4,9,10-perylenebis(discarboximide) [17].

Φ_{std} = 1 in chloroform

A_{std} = 0.1055

A_u = 0.1175

S_u = 1399.91

S_{std} = 4129.22

n_{std} = 1.446

n_u = 1.446

$$\Phi_f = \frac{0.1055}{0.1175} \times \frac{1399.91}{4129.22} \times \left[\frac{1.446}{1.446}\right]^2 \times 1$$

$\Phi_f = 0.30$

Similarly, the fluorescence quantum yield of Br-PDA in DMF was calculated and recorded in Table 4.1.

Table 4.1: Fluorescence Quantum Yield of Br-PDA and Decanol-PDA in Different Solvents

Compound	Solvent	Concentration (M)	Φ_f
Br-PDA	DMF	1×10^{-5}	0.57
Decanol-PDA	CHL	1×10^{-5}	0.30

4.2 Calculations of Molar Absorptivities (ε_{max})

The following equation (Beer-lamberts low) is used to calculate the molar absorptivities of the compounds [42].

$$\varepsilon_{\mathbf{max}} = \frac{A}{Cl}$$

Where,

ε_{max} : molar absorptivity in $L \bullet mol^{-1} \bullet cm^{-1}$ at λ_{max}

A : absorbance

c   : concentration in $mol \bullet L^{-1}$

l : cell length in cm

The ε_{max} Calculation of Decanol-PDA in CHL:
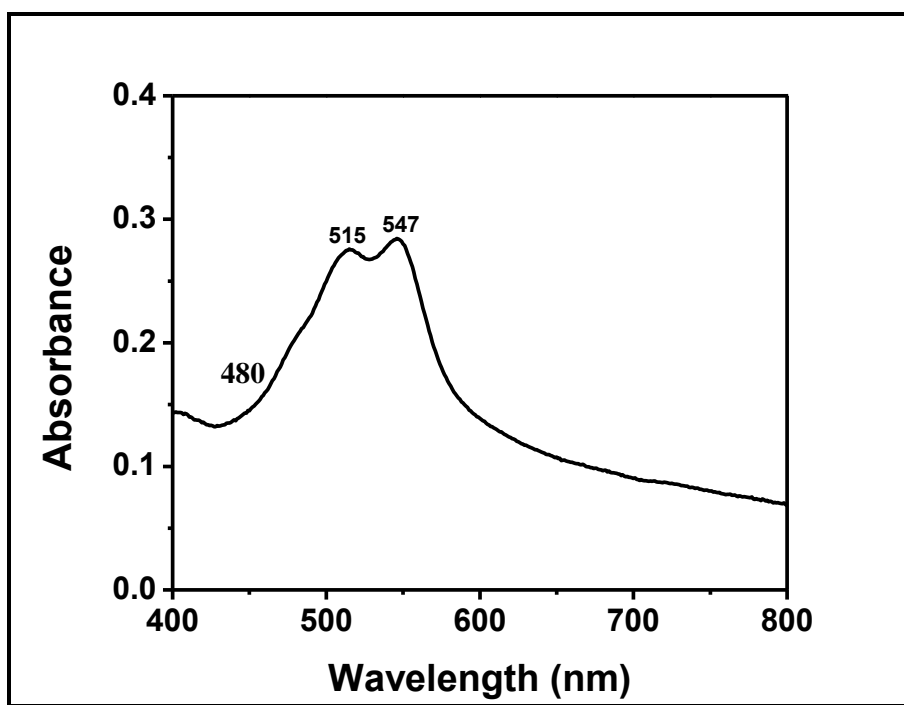
Figure 4.1: Absorbance Spectrum of Decanol-PDA in CHL at 1×10^{-5} M

In the Figure 4.1, at $\lambda_{max} = 547$ nm,

$A = 0.285$

$c = 1 \times 10^{-5}$ M

$l = 1$ cm

$\Rightarrow \varepsilon_{max} = \dfrac{A}{Cl} = \dfrac{0.285}{1 \times 10^{-5} \text{M} \times 1 \text{cm}} = 28500$ L • mol^{-1} • cm^{-1}

$\Rightarrow \varepsilon_{max}$ of Decanol-PDA $= 28500$ L • mol^{-1} • cm^{-1}

With the same way and equation, the molar absorptivities of PDA, Br-PDA and Decanol-PDA in different solvents were calculated and listed in the Table 4.2.

Table 4.2: Molar Absorptivities Data of Synthesized Compounds in Different Solvents

Compound	Solvent	Concentration (M)	A	λ_{max} (nm)	ε_{max} (M^{-1}. cm^{-1})
PDA	DMF	1×10^{-5}	0.210	517	21000
	DMSO	1×10^{-5}	0.570	522	57000
Br-PDA	DMF	1×10^{-5}	0.898	516	89800
	CHL	1×10^{-5}	0.990	520	99000
Decanol-PDA	DMF	1×10^{-5}	0.780	482	78000
	CHL	1×10^{-5}	0.285	547	28500
	MeOH	1×10^{-5}	0.325	509	32500

4.3 Full Width Half Maximum Calculations of Synthesized Compounds (FWHM, $\Delta\bar{\nu}_{1/2}$)

The full width at half maximum absorption is called a full width half maximum and can be calculated by the following equation [43].

$$\Delta\bar{\nu}_{1/2} = \bar{\nu}_I - \bar{\nu}_{II}$$

Where,

$\bar{\nu}_I$, $\bar{\nu}_{II}$: The frequencies from the absorption spectrum (cm^{-1})

$\Delta\bar{\nu}_{1/2}$: Half-width of the selected maximum absorption (cm^{-1})

$\Delta\bar{\nu}_{1/2}$ of Decanol-PDA in CHL:
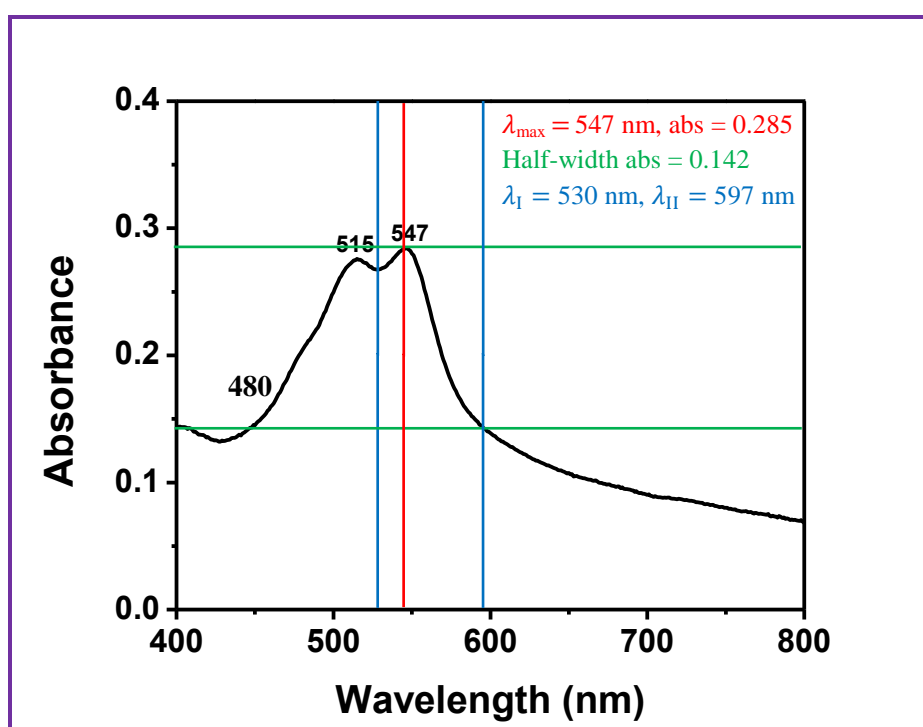

Figure 4.2: Absorbance Spectrum and FWHM Representation of Decanol-PDA in CHL at 1×10^{-5} M

From the Figure 4.2:

$\lambda_{max} = 547$ nm,   Half-width abs = 0.142

λ_I = 530 nm, λ_{II} = 597 nm

25

For $\lambda_I = 530$ nm

$$\Rightarrow \quad \lambda_I = 530 \text{ nm} \times \frac{10^{-9} \text{ m}}{1 \text{ nm}} \times \frac{1 \text{ cm}}{10^{-2} \text{ m}} = 5.30 \times 10^{-5} \text{ cm}$$

$$\Rightarrow \quad \bar{\nu}_I = \frac{1}{5.30 \times 10^{-5} \text{ cm}} = 18867.92 \text{ cm}^{-1}$$

For $\lambda_{II} = 597$ nm

$$\Rightarrow \quad \lambda_{II} = 597 \text{ nm} \times \frac{10^{-9} \text{ m}}{1 \text{ nm}} \times \frac{1 \text{ cm}}{10^{-2} \text{ m}} = 5.97 \times 10^{-5} \text{ cm}$$

$$\Rightarrow \quad \bar{\nu}_{II} = \frac{1}{5.97 \times 10^{-5} \text{ cm}} = 16750.42 \text{ cm}^{-1}$$

$$\Delta\bar{\nu}_{1/2} = \bar{\nu}_I - \bar{\nu}_{II} = 18867.92 \text{ cm}^{-1} - 16750.42 \text{ cm}^{-1} = 2117.5 \text{ cm}^{-1}$$

Similarly, the half-width of the selected maximum absorptions of the PDA, Br-PDA and Decanol-PDA in different solvents were calculated and recorded in Table 4.3.

Table 4.3: $\Delta\bar{\nu}_{1/2}$ Data of the Selected Absorptions of Synthesized Compounds in Different Solvents

Compound	Solvent	Concentration (M)	λ_{max} (nm)	λ_I (nm)	λ_{II} (nm)	$\Delta\bar{\nu}_{1/2}$ (cm^{-1})
PDA	DMF	1×10^{-5}	517	497	546	1805.7
	DMSO	1×10^{-5}	522	496	544	1778.9
Br-PDA	DMF	1×10^{-5}	516	500	541	1515.7
	CHL	1×10^{-5}	520	500	536	1343.3
Decanol-PDA	DMF	1×10^{-5}	482	450	508	2537.2
	CHL	1×10^{-5}	547	530	597	2117.5
	MeOH	1×10^{-5}	509	425	604	6973.1

4.4 Theoretical Radiative Lifetime Data (τ_0)

The theoretical radiative lifetime of an excited molecule can be calculated from the following equation [43]:

$$\tau_0 = \frac{3.5 \times 10^8}{\bar{v}_{max}^2 \times \varepsilon_{max} \times \Delta\bar{v}_{1/2}}$$

Where,

τ_0 : Theoretical radiative lifetime (s)

$\bar{v}_{max}$: Frequency of the maximum absorption band (cm^{-1})

ε_{max} : Molar absorptivity in L $\bullet$ mol^{-1} $\bullet$ cm^{-1} at λ_{max}

$\Delta\bar{v}_{1/2}$: Full width half maximum of the selected maximum absorption (cm^{-1})

τ_0 of Decanol-PDA in CHL:

With the help of calculated ε_{max} and $\Delta\bar{v}_{1/2}$ values for the selected absorptions of Decanol-PDA, τ_0 was calculated as:

From the Figures 4.1 and 4.2, $\lambda_{max} = 547$

$$\lambda_{max} = 547 \text{ nm} \times \frac{10^{-9}\text{m}}{1 \text{ nm}} \times \frac{1\text{cm}}{10^{-2}\text{m}} = 5.47 \times 10^{-5} \text{ cm}$$

$$\Rightarrow \quad \bar{v}_{max} = \frac{1}{5.47\times10^{-5} \text{ cm}} = 18281.5 \text{ cm}^{-1}$$

$$\Rightarrow \quad \bar{v}_{max}^2 = (18281.5 \text{ cm}^{-1})^2 = 3.34 \times 10^8 \text{ (cm}^{-1})^2$$

Now, from the above-mentioned equation, the theoretical radiative lifetime of compounds can be calculated:

$$\tau_0 = \frac{3.5 \times 10^8}{\bar{v}_{max}^2 \times \varepsilon_{max} \times \Delta\bar{v}_{1/2}} = \frac{3.5 \times 10^8}{3.34 \times 10^8 \times 28500 \times 2117.5} = 1.74 \times 10^{-8} \text{ s}$$

$\Rightarrow \quad \boldsymbol{\tau}_0 = 17.4$ ns

Likewise, the theoretical radiative lifetimes of the PDA, Br-PDA and Decanol-PDA in different solvents were calculated and the data were listed in Table 4.3.

Table 4.4: τ_0 Values of Synthesized Compounds in Different Solvents at 1×10^{-5} M

Compound	Solvent	λ_{max} (nm)	ε_{max} (M^{-1} cm^{-1})	$\bar{v}_{max}^2$ (cm^{-2})	$\Delta\bar{v}_{1/2}$ (cm^{-1})	τ_0 (ns)
PDA	DMF	517	21000	3.74×10^8	1805.7	24.7
	DMSO	522	57000	3.67×10^8	1778.9	9.4
Br-PDA	DMF	516	89800	3.76×10^8	1515.7	6.8
	CHL	520	99000	3.70×10^8	1343.3	7.1
Decanol-PDA	DMF	482	78000	4.30×10^8	2537.2	4.1
	CHL	547	28500	3.34×10^8	2117.5	17.4
	MeOH	509	32500	1.88×10^8	6973.1	4.0

4.5 Theoretical Fluorescence Lifetime Data (τ_f)

Theoretical fluorescence lifetime of the molecule is the theoretical average time staying in the excited state before emitting a photon (fluorescence), and calculated by following equation [43]:

$$\tau_f = \tau_0 \cdot \Phi_f$$

Where, τ_f : Theoretical fluorescence lifetime in (ns)

   τ_0 : Theoretical radiative lifetime (ns)

   Φ_f : Fluorescence quantum yield

The τ_f Calculation of Decanol-PDA in CHL:

$\tau_f = \tau_0 \cdot \Phi_f$

$\tau_f = 17.4 \times 0.30$

$\tau_f = 5.22$ ns

Similarly, the theoretical fluorescence lifetime of Br-PDA in DMF was calculated and recorded in Table 4.5.

Table 4.5: Theoretical Fluorescence Lifetime of Br-PDA and Decanol-PDA in Different Solvents

Compound	Solvent	Concentration (M)	τ_0 (ns)	Φ_f	τ_f (ns)
Br-PDA	DMF	1×10^{-5}	6.8	0.57	3.88
Decanol-PDA	CHL	1×10^{-5}	17.4	0.30	5.22

4.6 Calculation of Fluorescence Rate Constants (k_f)

The theoretical k_f of the synthesized compounds can be calculated by the equation [43]:

$$k_f = \frac{1}{\tau_0}$$

Where,

k_f : Fluorescence rate constant (s^{-1})

τ_0 : Theoretical radiative lifetime (s)

The Fluorescence Rate Constant of Decanol-PDA in CHL:

$$\Rightarrow k_f = \frac{1}{1.74 \times 10^{-8} \text{ s}} = 5.75 \times 10^7 \text{ s}^{-1}$$

$$\Rightarrow k_f = 5.75 \times 10^7 \text{ s}^{-1}$$

The fluorescence rate constant of PDA, Br-PDA and Decanol-PDA in different solvents were calculated in the similar methods and the data were listed in Table 4.6.

Table 4.6: k_f of Synthesized Compounds in Different Solvents

Compound	Solvent	Concentration (M)	τ_0 (ns)	k_f (s^{-1})
PDA	DMF	1×10^{-5}	24.7	4.05×10^7
	DMSO	1×10^{-5}	9.4	1.06×10^8
Br-PDA	DMF	1×10^{-5}	6.8	1.47×10^8
	CHL	1×10^{-5}	7.1	1.41×10^8
Decanol-PDA	DMF	1×10^{-5}	4.1	2.44×10^8
	CHL	1×10^{-5}	17.4	5.75×10^7
	MeOH	1×10^{-5}	4.0	2.50×10^8

4.7 Calculations of Oscillator Strengths (f)

The oscillator strength is an electronic transition strength that extracted by dimensionless quantity. It can be calculated from the following equation [43]:

$$f = 4.32 \times 10^{-9} \times \Delta \bar{\nu}_{1/2} \; \varepsilon_{max}$$

Where,

f : Oscillator Strength

$\Delta \bar{\nu}_{1/2}$: Half-width of the Selected Absorption in cm^{-1}

ε_{max} : Maximum molar absorptivity in L • mol^{-1} • cm^{-1} at maximum

         wavelength (λ_{max})

The Oscillator Strength of Decanol-PDA in CHL:

$\Rightarrow$ $= 4.32 \times 10^{-9} \times \Delta \bar{\nu}_{1/2} \; \varepsilon_{max}$

$\Rightarrow$ $= 4.32 \times 10^{-9} \times 2117.5 \times 28500$

$\Rightarrow f = 0.26$

The oscillator strength of the radiationless deactivation for PDA, Br-PDA and Decanol-PDA in different solvents were calculated and listed in the following table (Table 4.7).

Table 4.7: f of Synthesized Compounds in Different Solvents at 1×10^{-5} M

Compound	Solvent	λ_{max} (nm)	ε_{max} (M^{-1}cm^{-1})	$\Delta\bar{\nu}_{1/2}$ (cm^{-1})	f
PDA	DMF	517	21000	1805.7	0.16
	DMSO	522	57000	1778.9	0.44
Br-PDA	DMF	516	89800	1515.7	0.59
	CHL	520	99000	1343.3	0.57
Decanol-PDA	DMF	482	78000	2537.2	0.85
	CHL	547	28500	2117.5	0.26
	MeOH	509	32500	6973.1	0.98

4.8 Calculations of Singlet Energies (E_s)

The amount of energy required to excite one electron from the ground state to the excited state of chromophore is called singlet energy [43].

$$E_s = \frac{2.86 \times 10^5}{\lambda_{max}}$$

Where,

E_s : singlet energy in kcal . mol^{-1}

λ_{max} : the maximum absorbance wavelength in $\overset{\circ}{A}$

Singlet Energy of Decanol-PDA in CHL:

$$E_s = \frac{2.86 \times 10^5}{\lambda_{max}} = \frac{2.86 \times 10^5}{5470} = 52.3 \text{ kcal . mol}^{-1}$$

$E_s = 52.3$ kcal . mol^{-1}

With the same way, the singlet energies of PDA, Br-PDA and Decanol-PDA were calculated and listed in the Table 4.8.

Table 4.8: E_s of the Synthesized Compounds in Different Solvents at 1×10^{-5} M

Compound	Solvent	λ_{max} ($\overset{\circ}{A}$)	E_s (kcal . mol^{-1})
PDA	DMF	5170	55.3
	DMSO	5220	54.8
Br-PDA	DMF	5160	55.4
	CHL	5200	55.0
Decanol-PDA	DMF	4820	59.3
	CHL	5470	52.3
	MeOH	5090	56.2

4.9 Calculation of Optical Band Gap Energies (E_g)

The measurement of the optical band gap energies of materials can be calculated from the following equation [43]:

$$E_g = \frac{1240 \text{ eV nm}}{\lambda}$$

Where,

E_g : energy band gap in units of eV

λ : cut-off wavelength of the absorption band in units of nm

The band gap energy of Decanol-PDA in CHL:

From the maximum absorption band, the cut-off wavelength of the absorption band ($0\rightarrow0$ absorption band) can be estimated by induction it to zero.
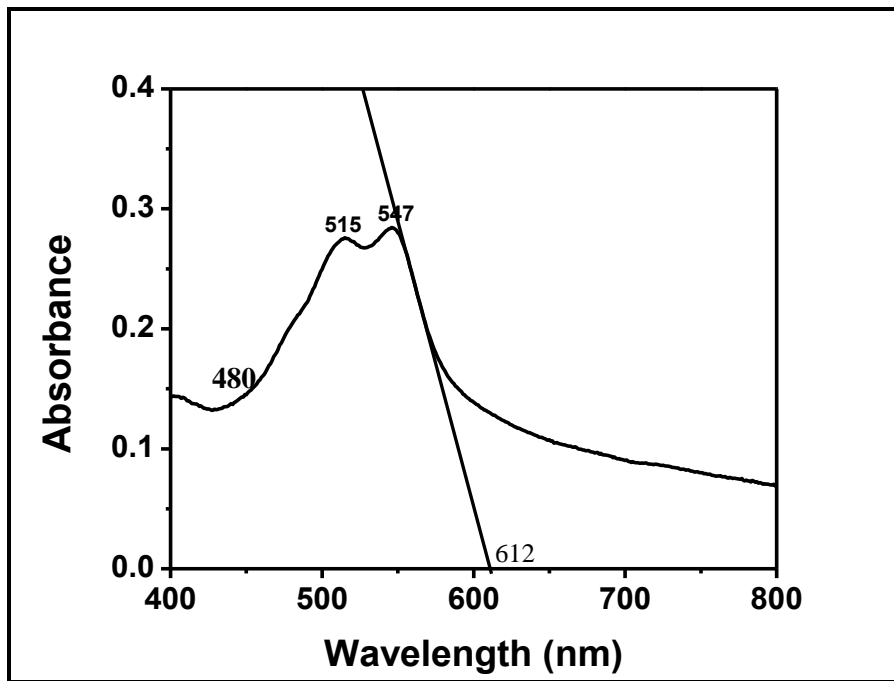

Figure 4.3: Absorbance Spectrum of Decanol-PDA in CHL and the Cut-Off Wavelength

$$E_g = \frac{1240 \text{ eV nm}}{\lambda}$$

$$\Rightarrow E_g = \frac{1240 \text{ eV nm}}{\lambda} = \frac{1240 \text{ eV nm}}{612} = 2.03 \text{ eV}$$

$$\Rightarrow E_g = 2.03 \text{ eV}$$

The band gap energies of PDA, Br-PDA and Decanol-PDA in different solvents were calculated in the similar ways that used above and the data listed in the following table (Table 4.9).

Table 4.9: Band Gap Energies Data of Synthesized Compounds in Different Solvents

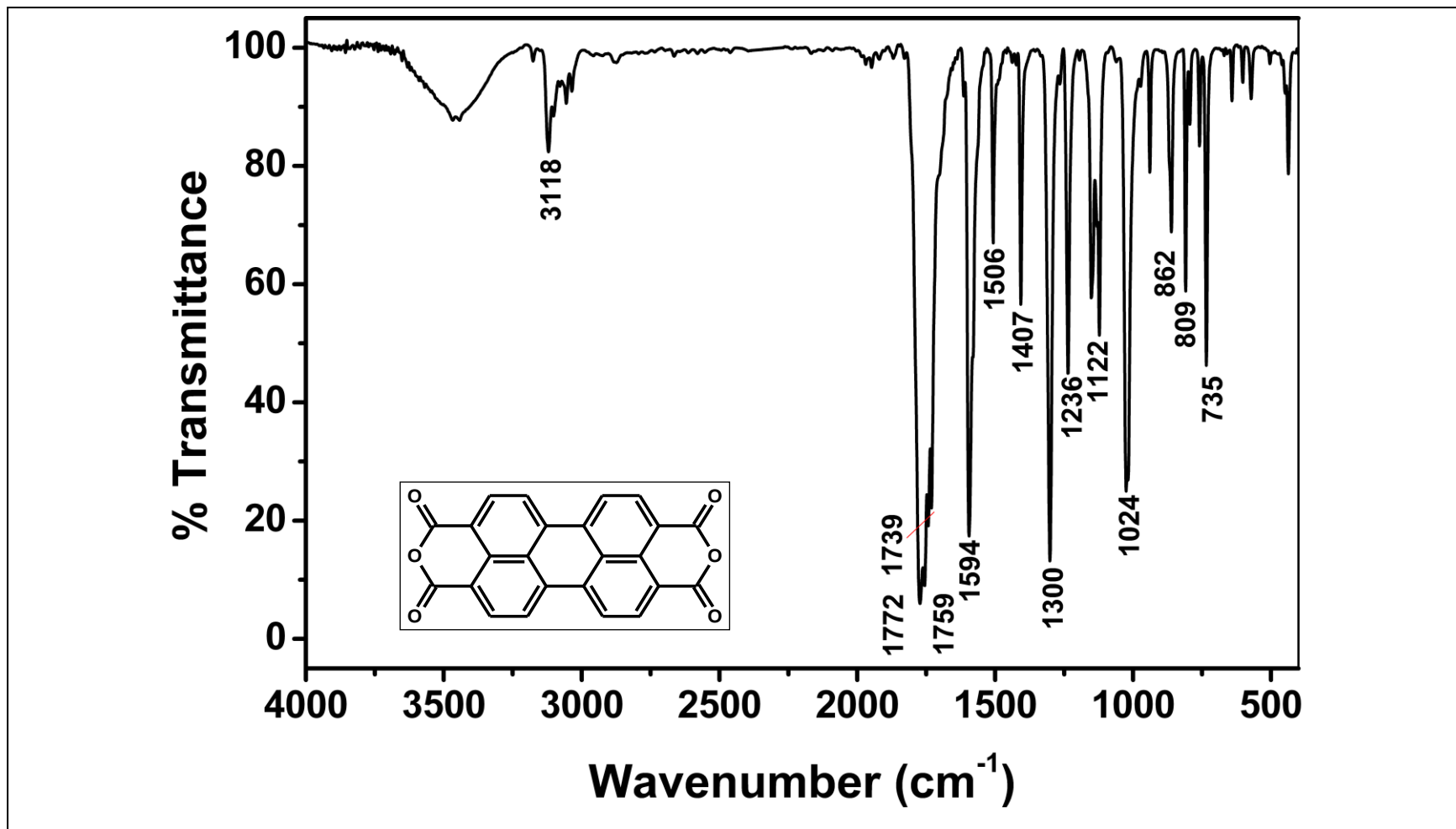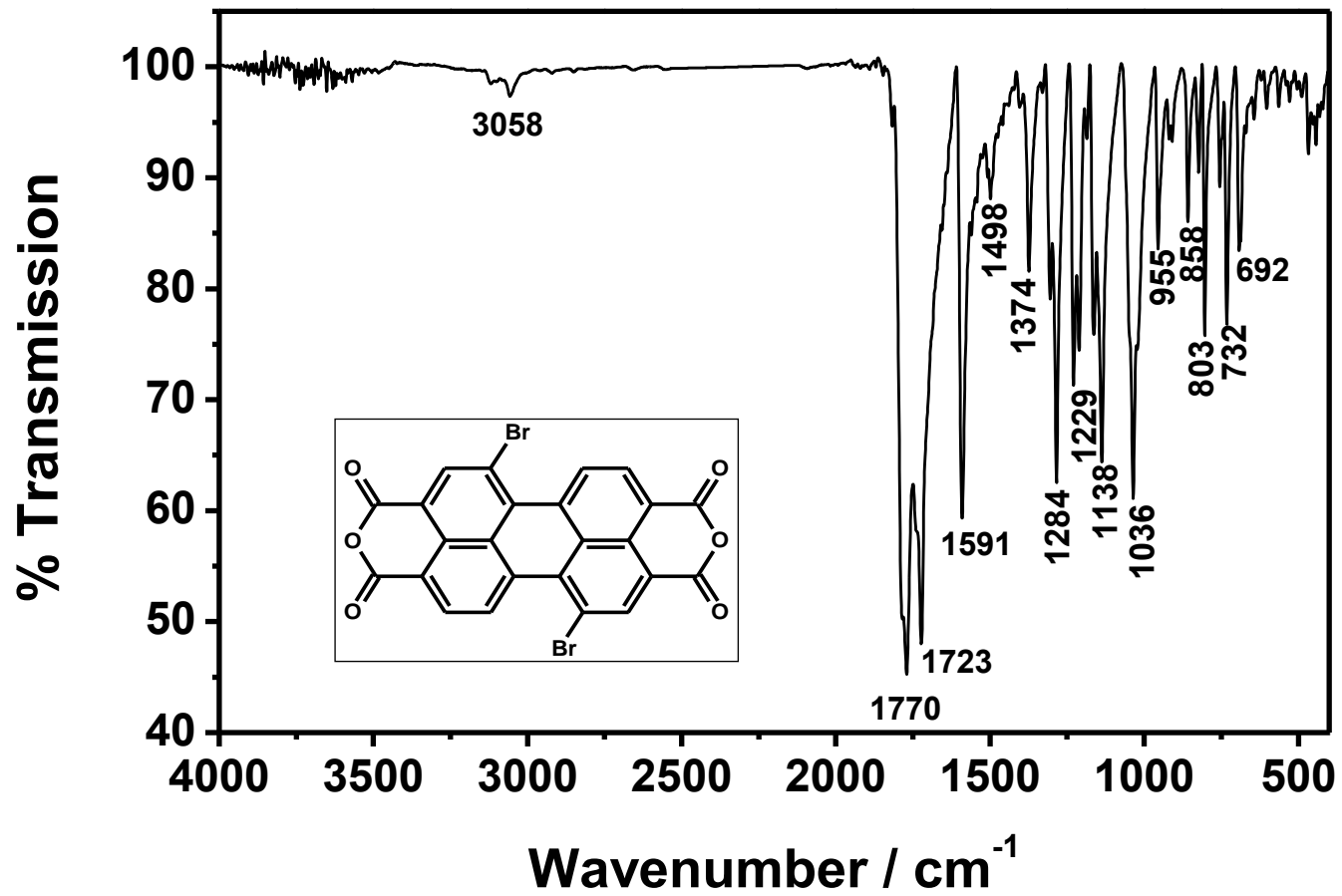| Compound	Solvent	Concentration (M)	λ_{max} (nm)	Cut-off λ	E_g (eV)
PDA	DMF	1×10^{-5}	517	600	2.07
	DMSO	1×10^{-5}	522	736	1.68
Br-PDA	DMF	1×10^{-5}	516	556	2.23
	CHL	1×10^{-5}	520	545	2.28
Decanol-PDA	DMF	1×10^{-5}	482	662	1.87
	CHL	1×10^{-5}	547	612	2.03
	MeOH	1×10^{-5}	509	636	1.95

Figure 4.4: FTIR Spectrum of PDA
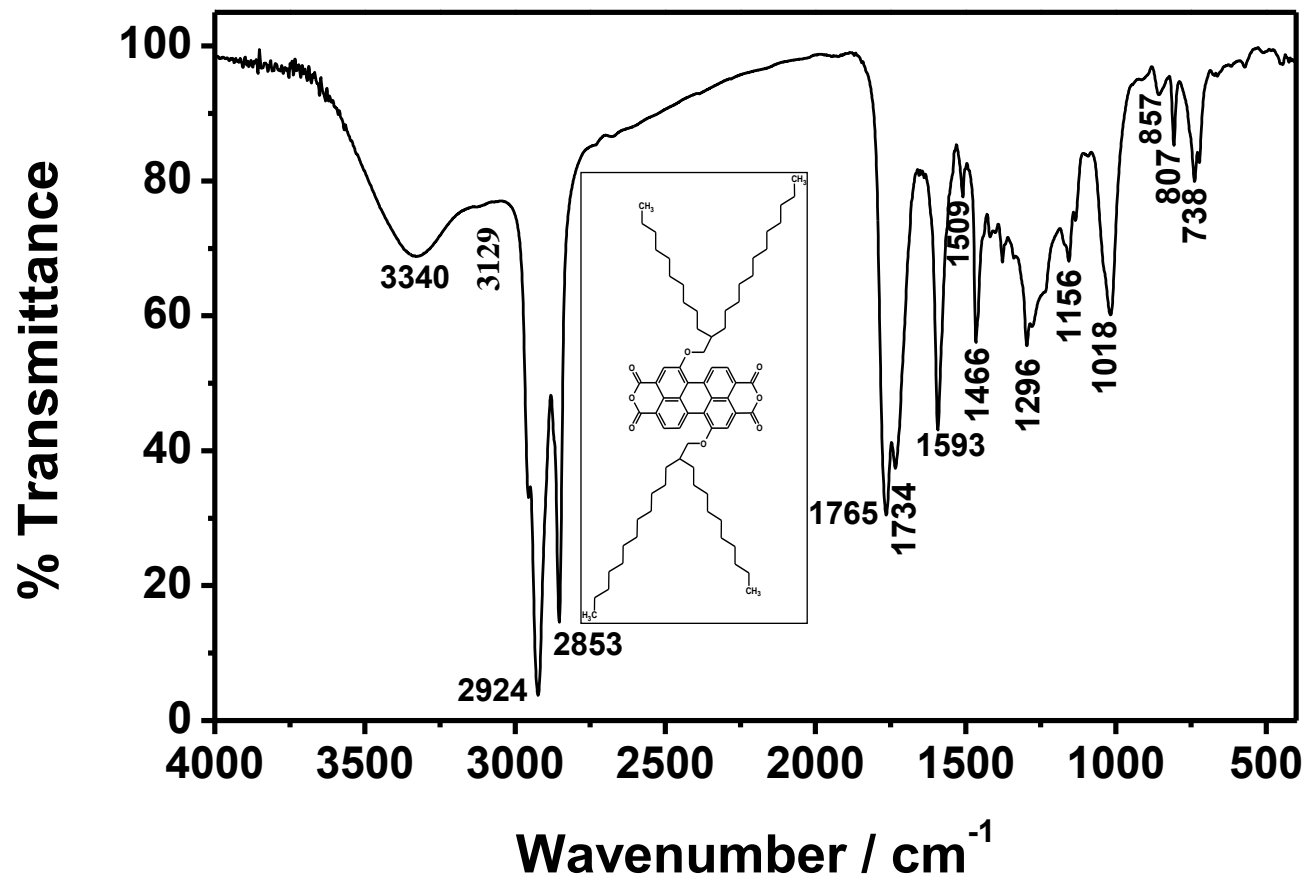
Figure 4.5: FTIR Spectrum of Br-PDA

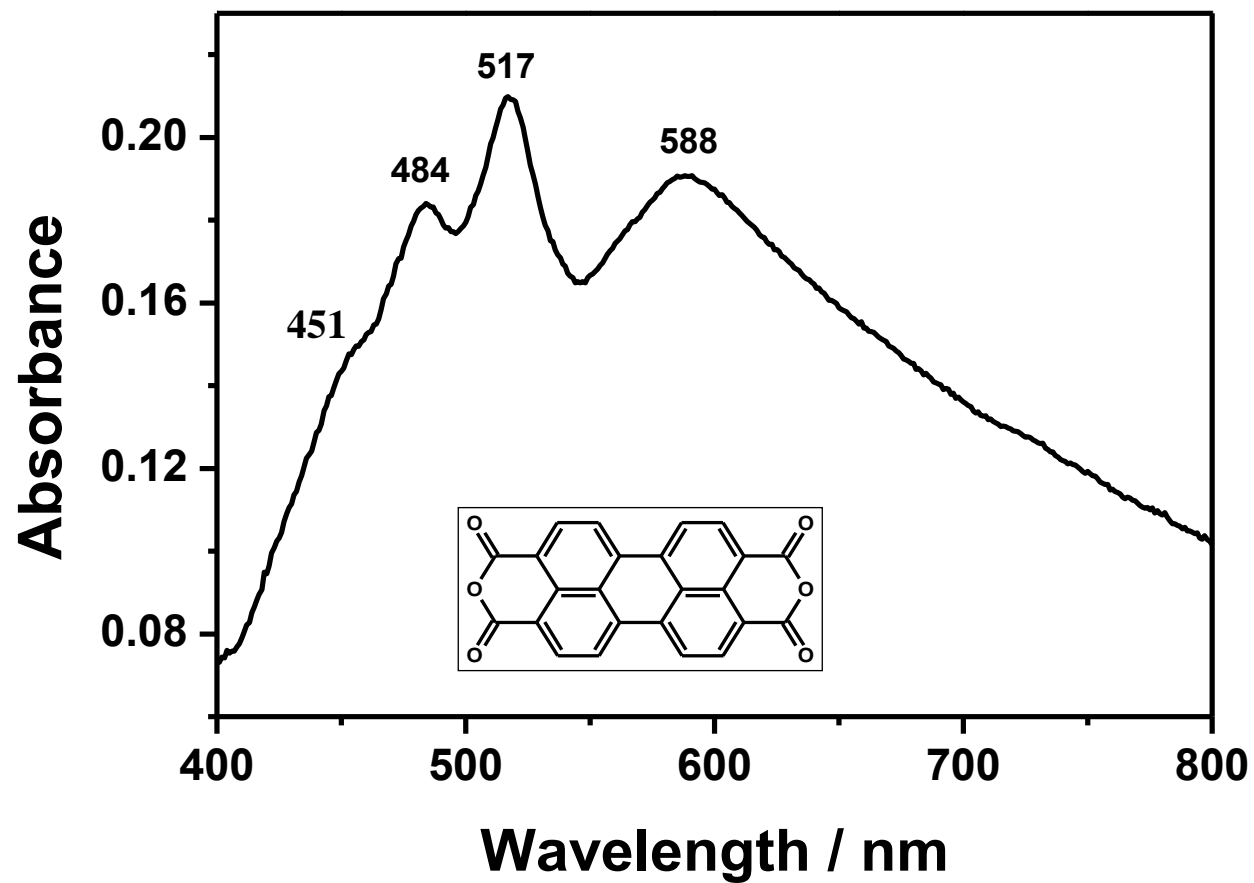Figure 4.6: FTIR Spectrum of Decanol-PDA

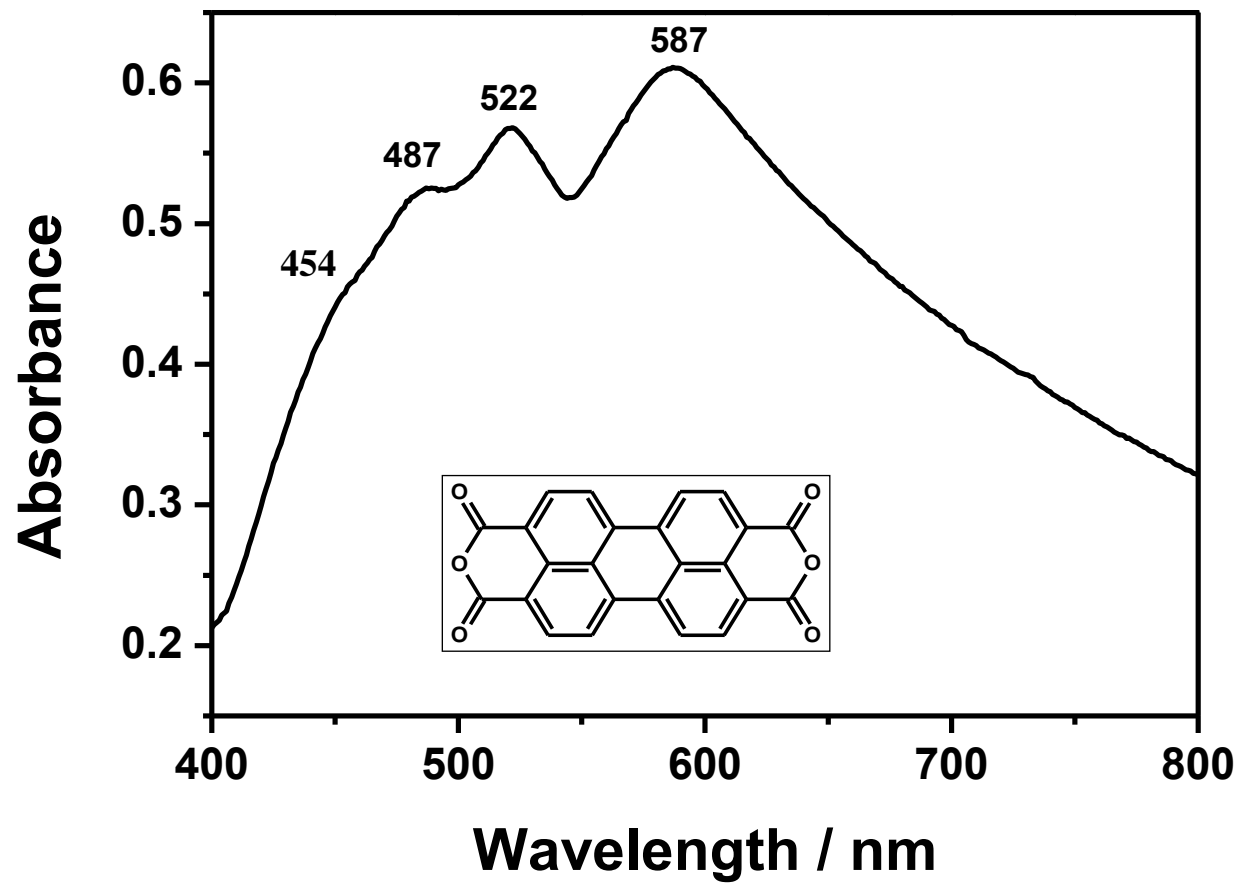Figure 4.7: Absorbance Spectrum of PDA in DMF
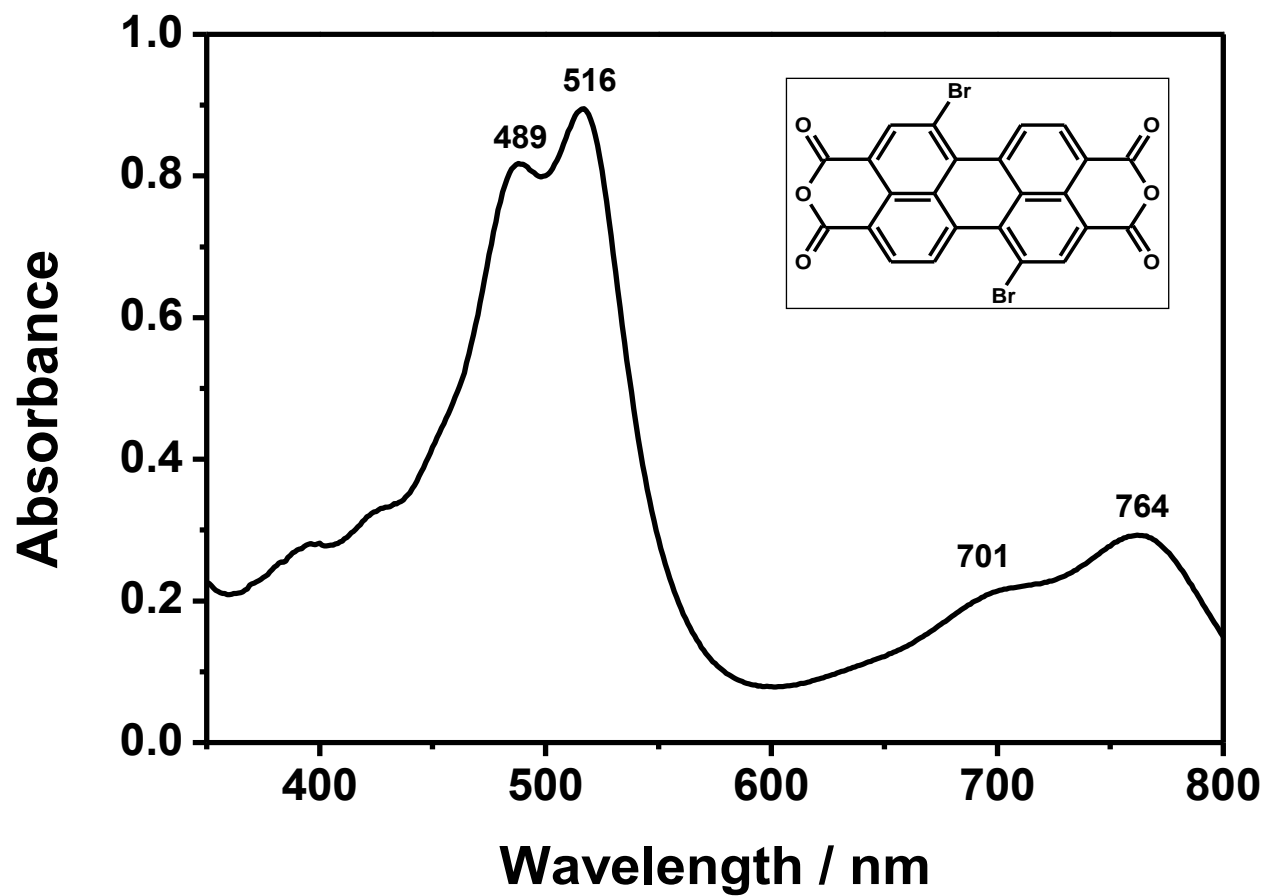
Figure 4.8: Absorbance Spectrum of PDA in DMSO

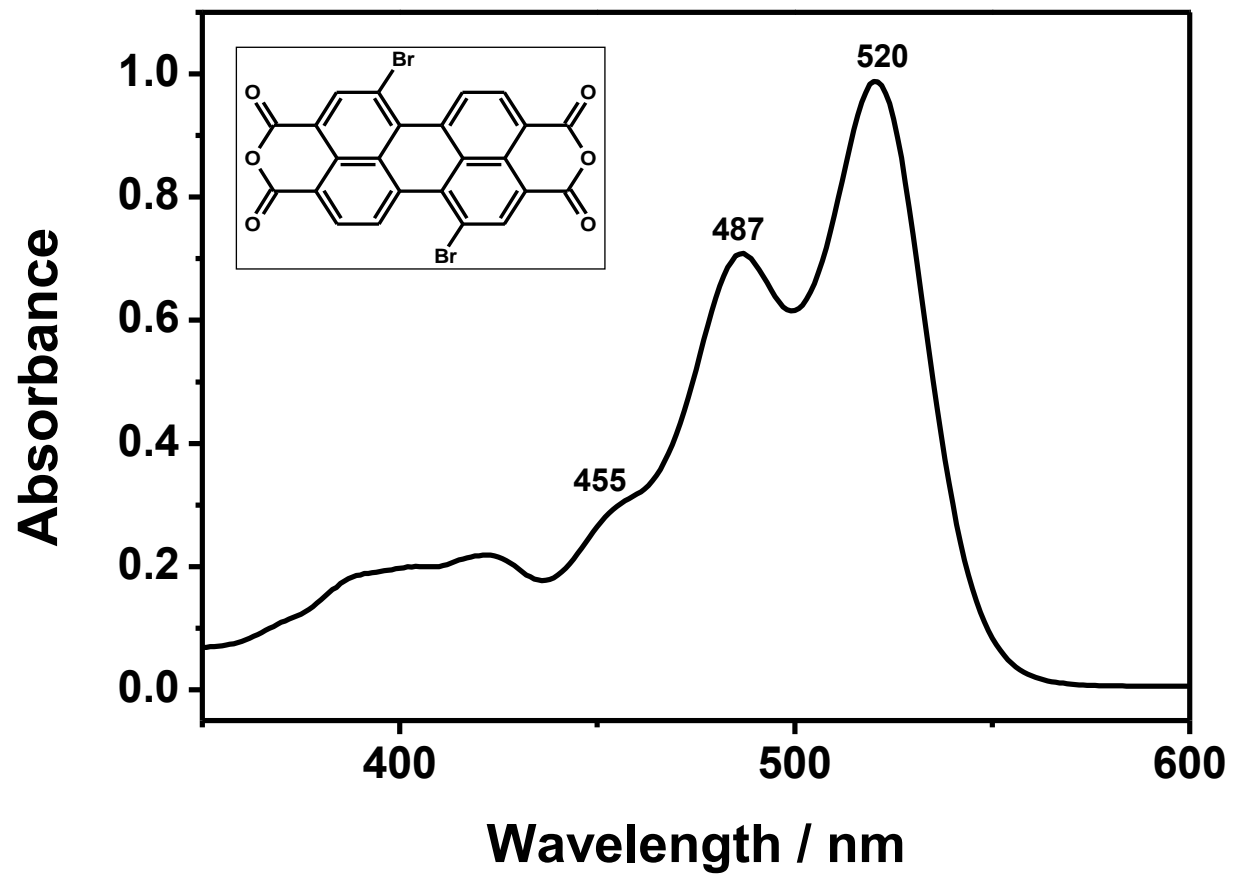Figure 4.9: Absorbance Spectrum of Br-PDA in DMF

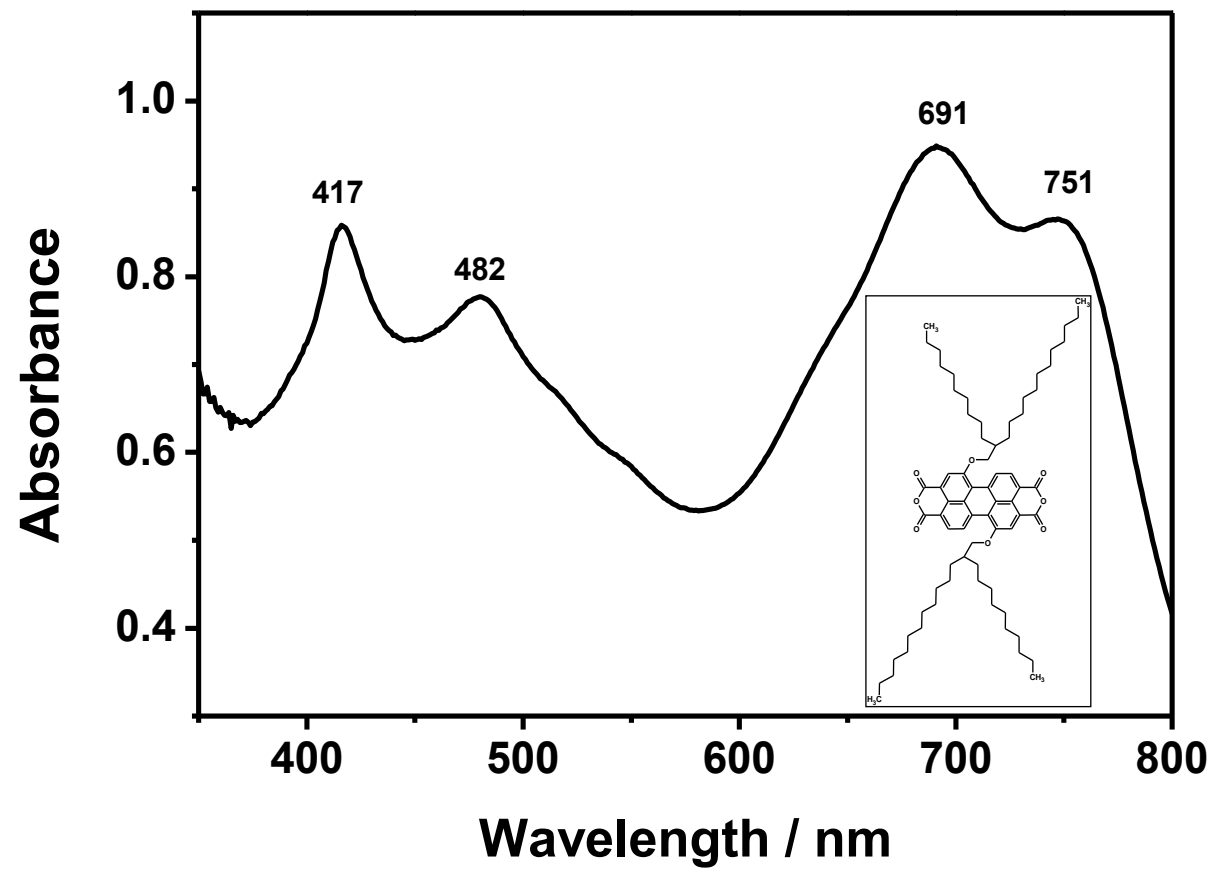Figure 4.10: Absorbance Spectrum of Br-PDA in CHL

Figure 4.11: Absorbance Spectrum of Decanol-PDA in DMF
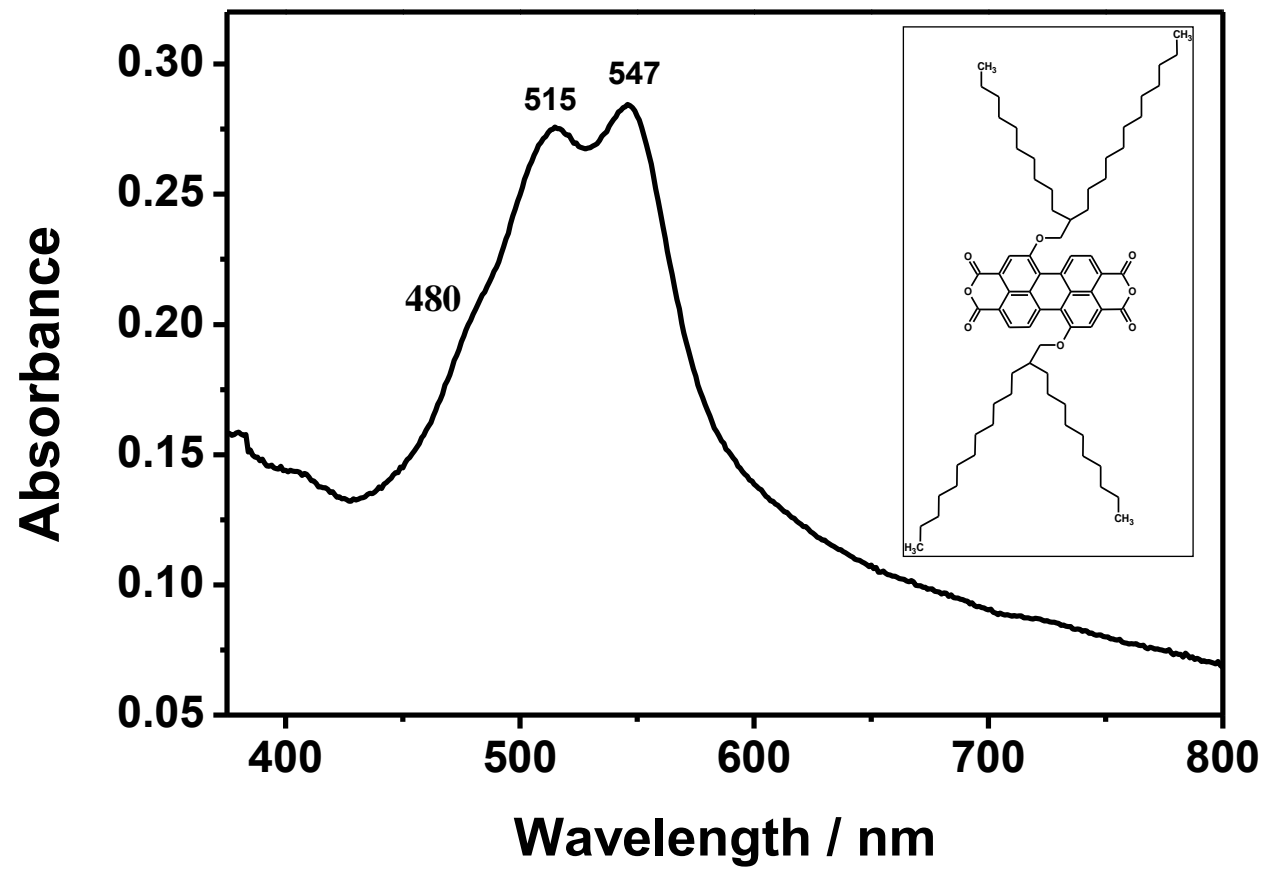
Figure 4.12: Absorbance Spectrum of Decanol-PDA in CHL
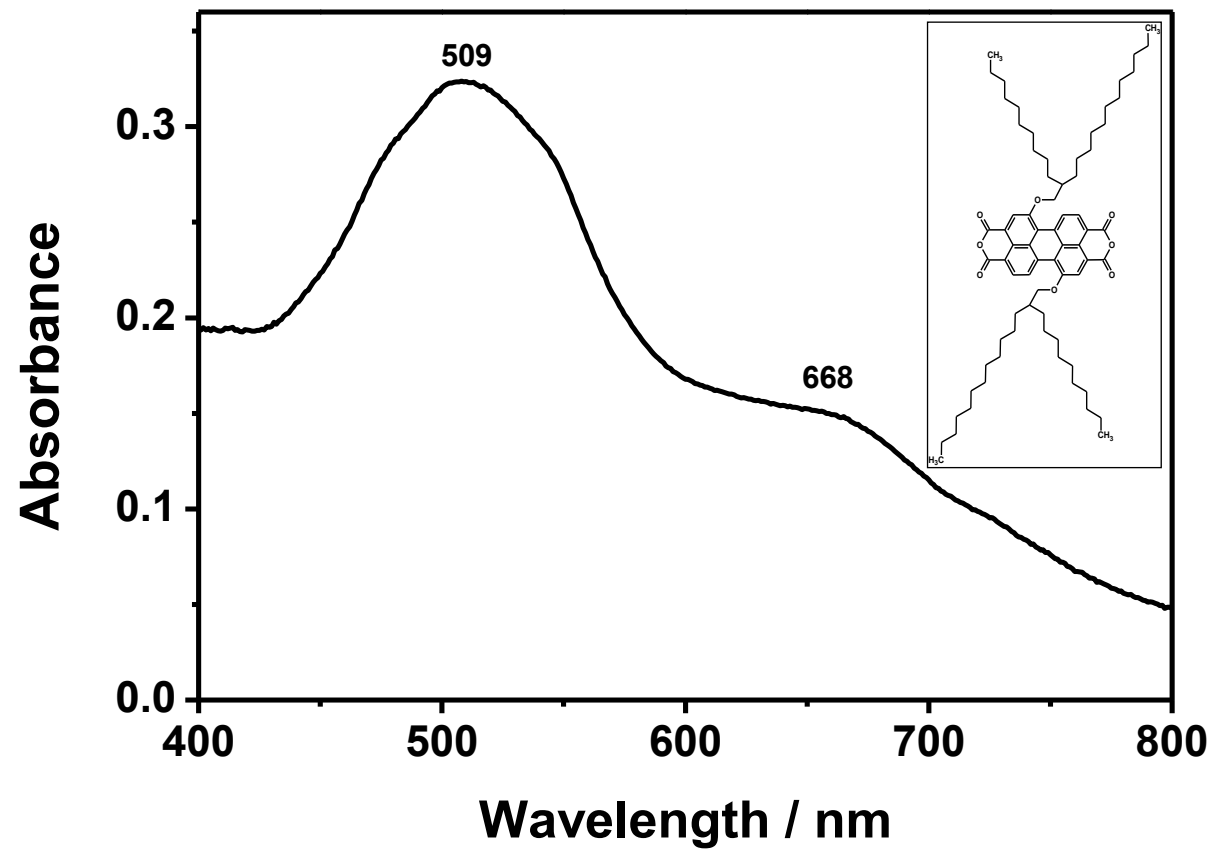
Figure 4.13: Absorbance Spectrum of Decanol-PDA in MeOH
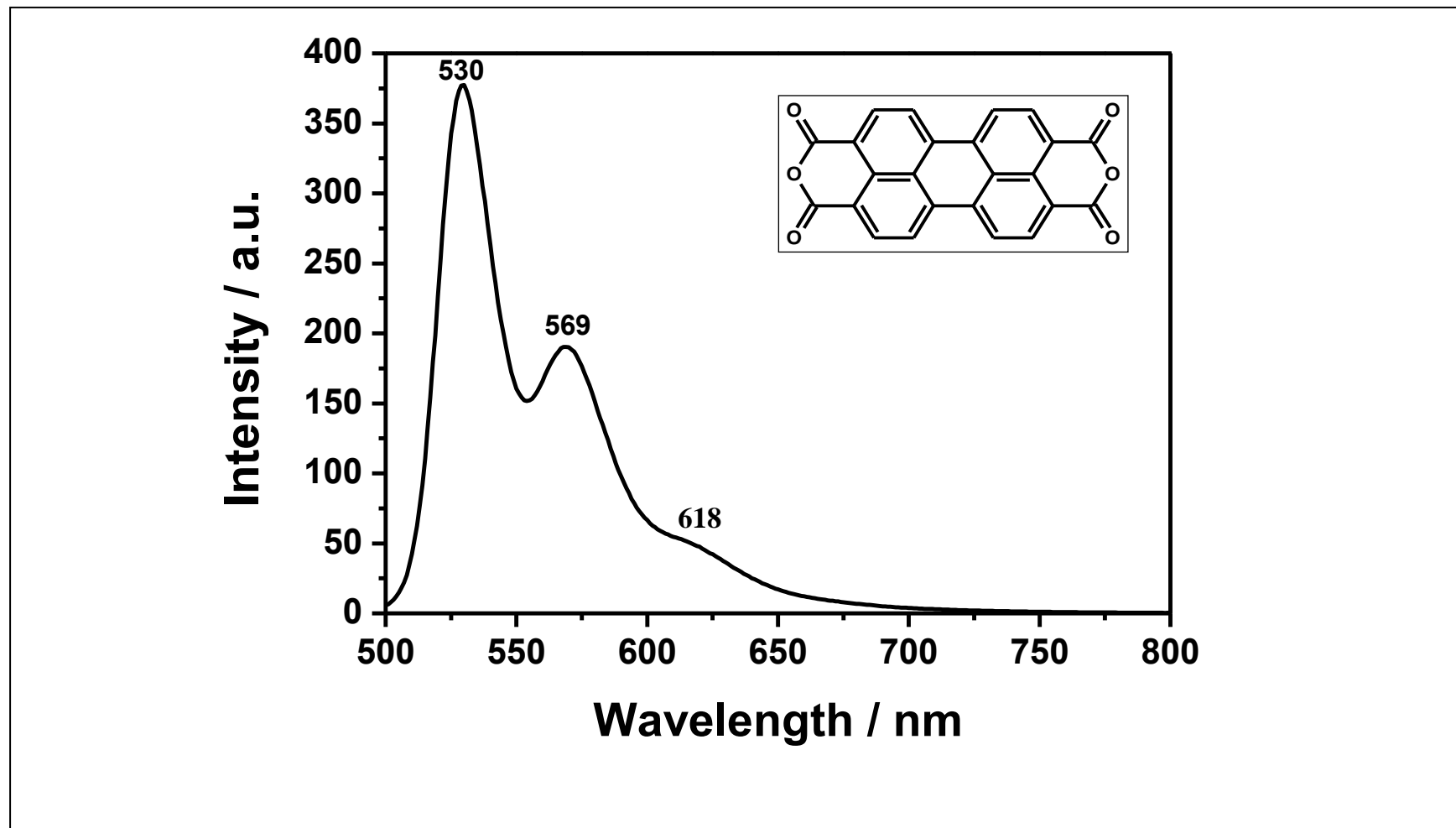
Figure 4.14: Emission Spectrum of PDA in DMF at $\lambda_{exc} = 485$ nm
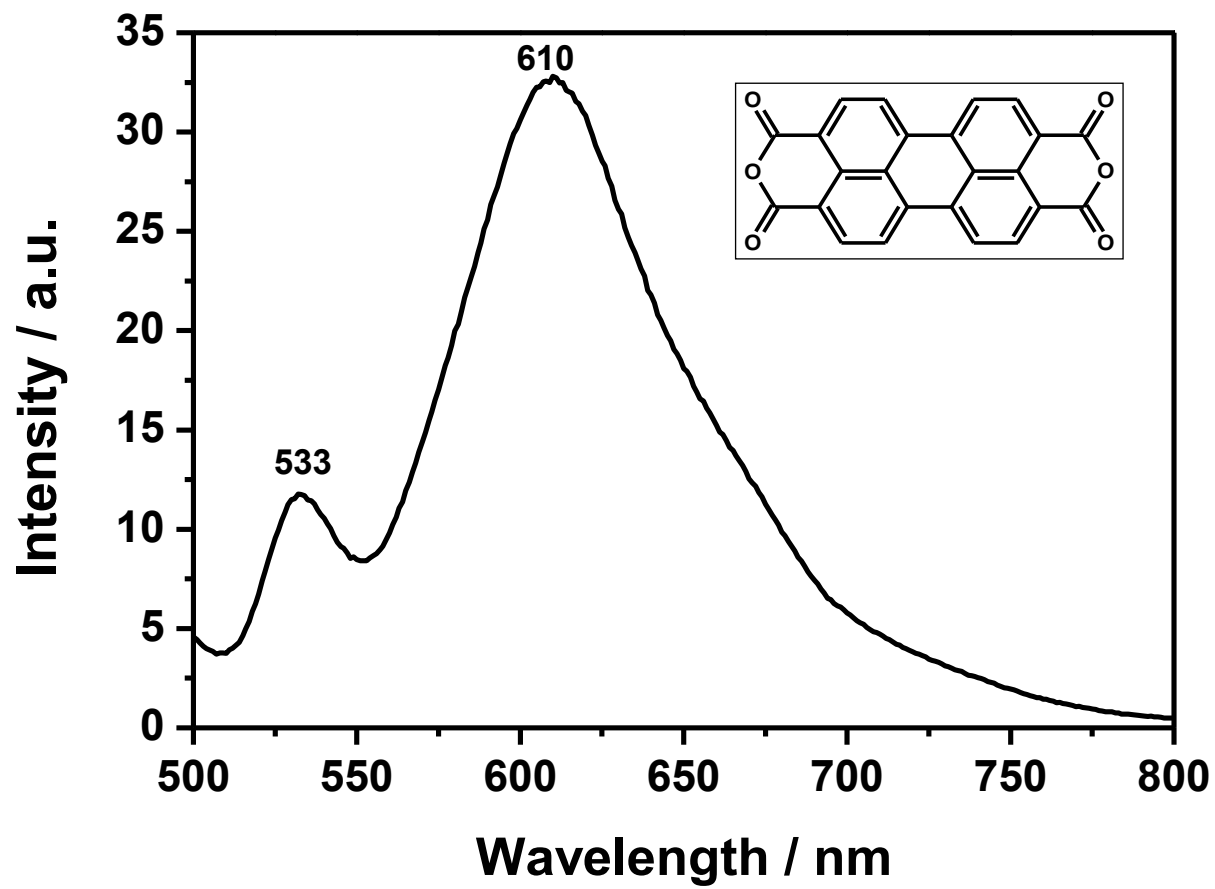
Figure 4.15: Emission Spectrum of PDA in DMSO at $\lambda_{exc} = 485$ nm
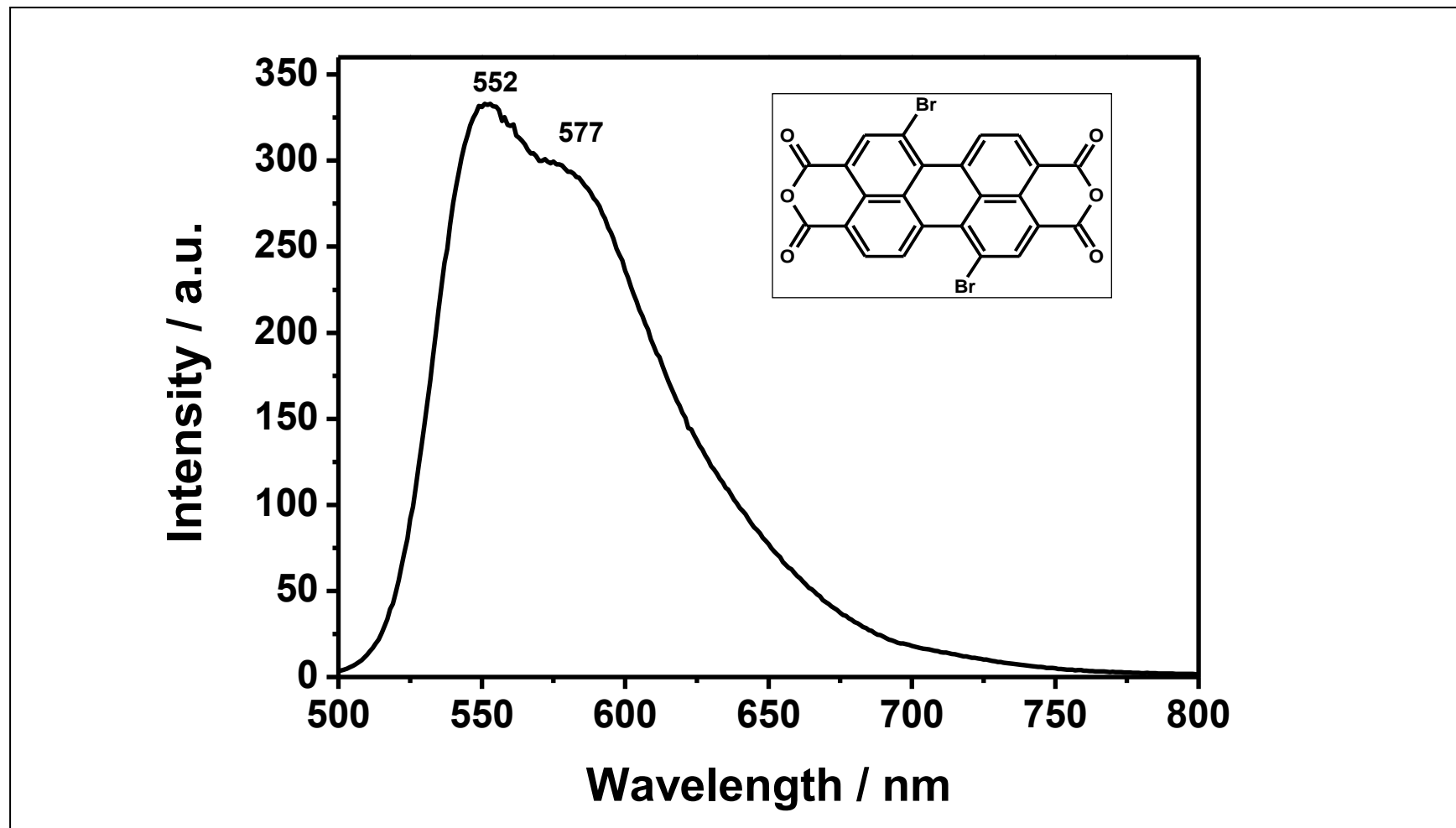
Figure 4.16: Emission Spectrum of Br-PDA in DMF at $\lambda_{exc} = 485$ nm

Figure 4.17: Emission Spectrum of Br-PDA in CHL at λ_{exc} = 485 nm

Figure 4.18: Emission Spectrum of Decanol-PDA in DMF at $\lambda_{exc} = 485$ nm

Figure 4.19: Emission Spectrum of Decanol-PDA in CHL at $\lambda_{exc} = 485$ nm
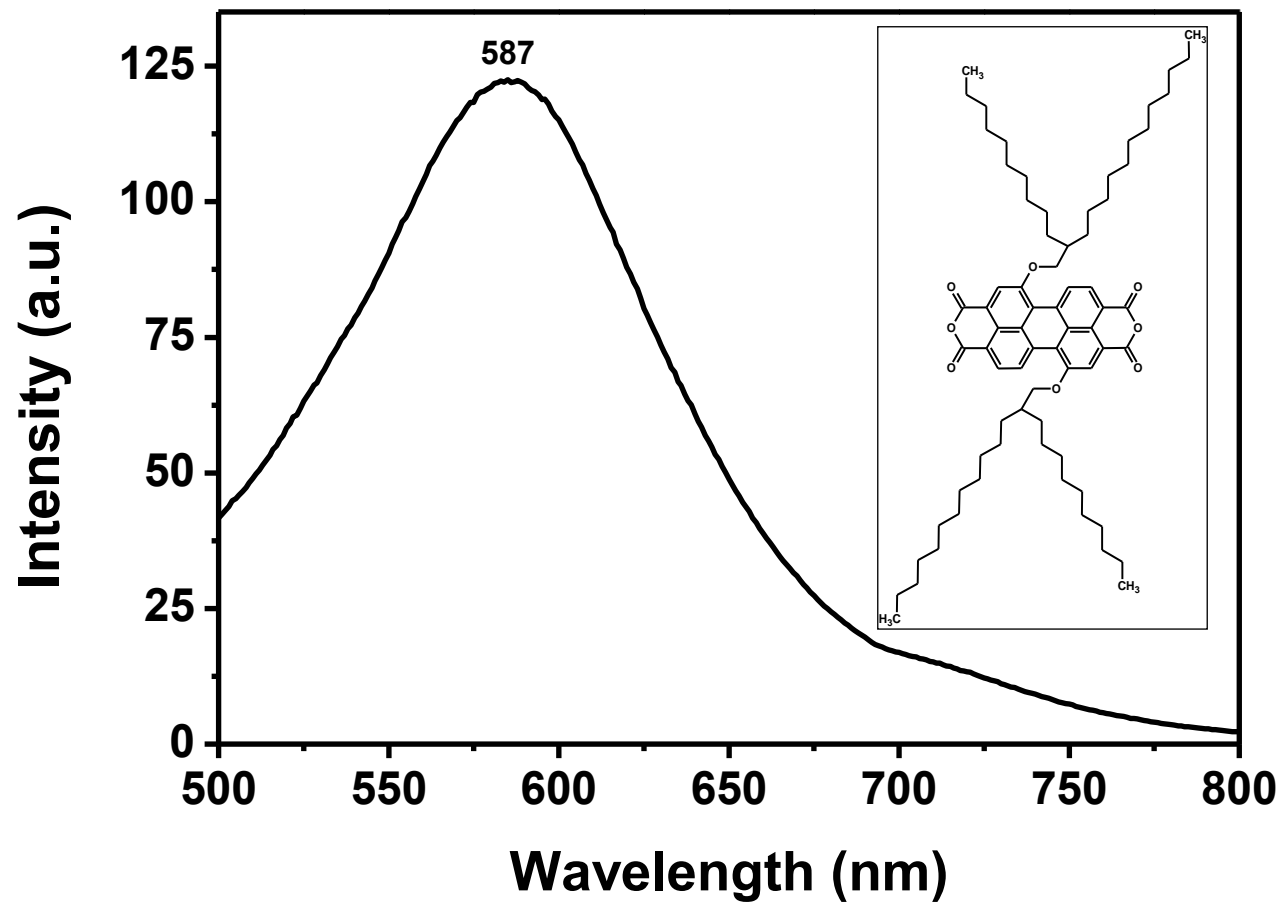
Figure 4.20: Emission spectrum of Decanol-PDA in MeOH at $\lambda_{exc} = 485$ nm
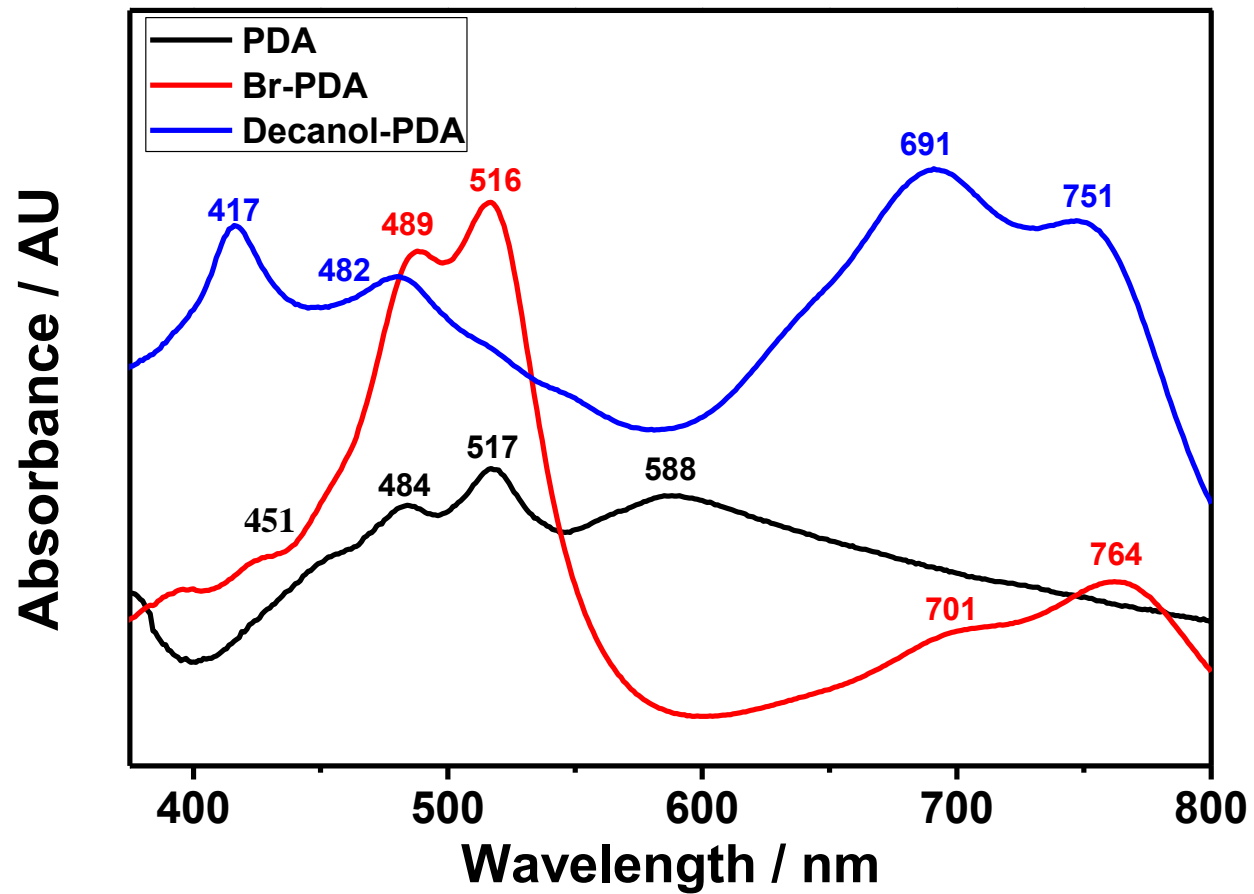
Figure 4.21: Absorbance spectra of PDA, Br-PDA and Decanol-PDA in DMF
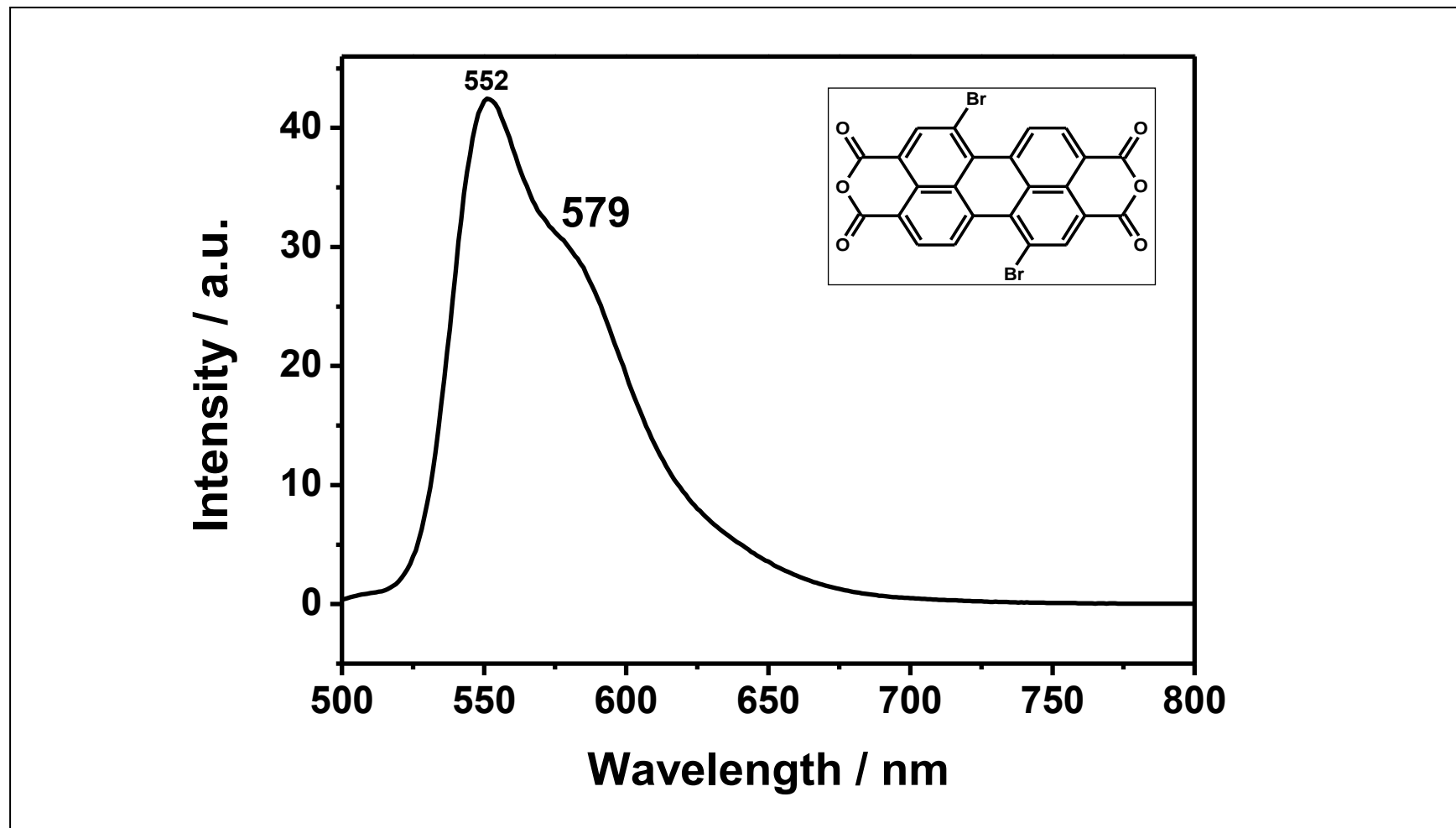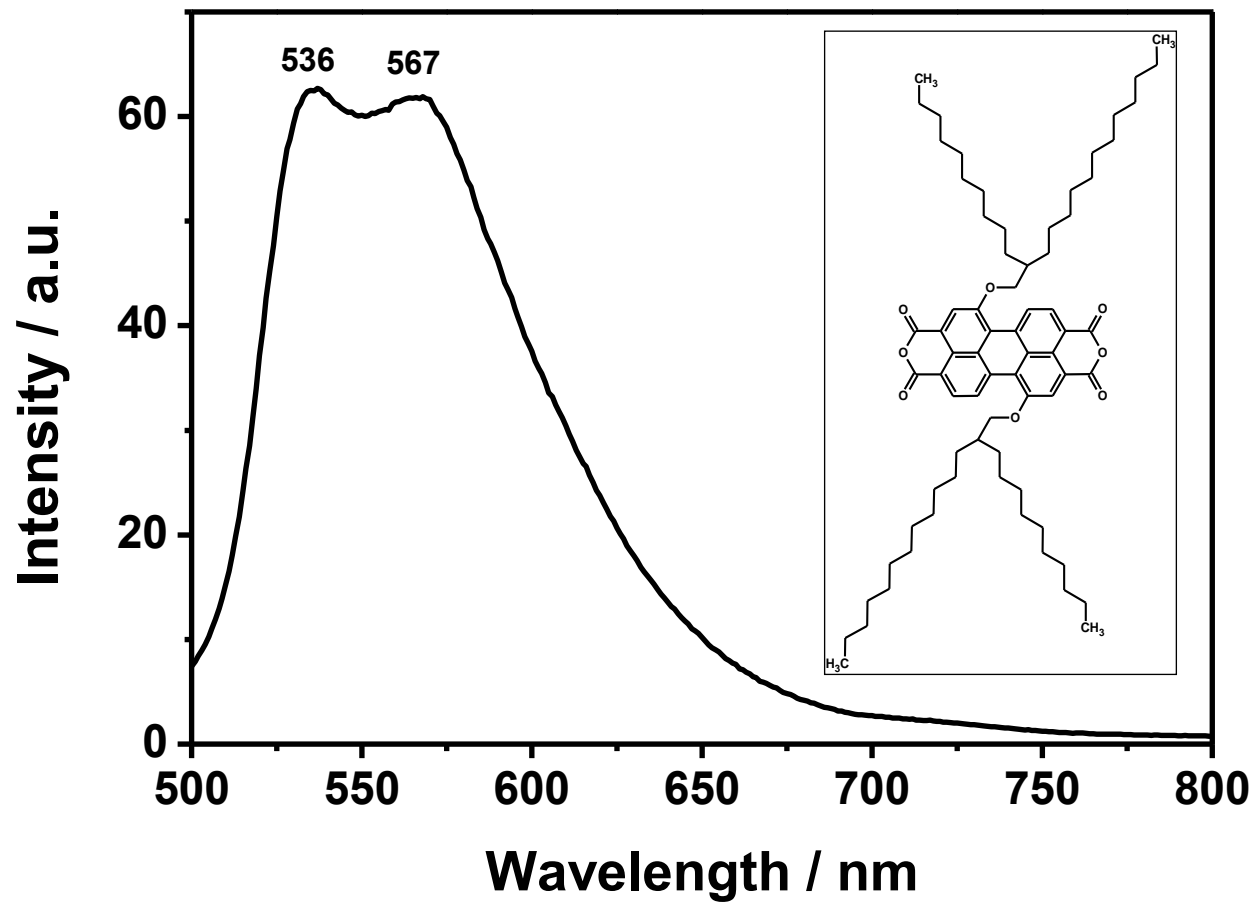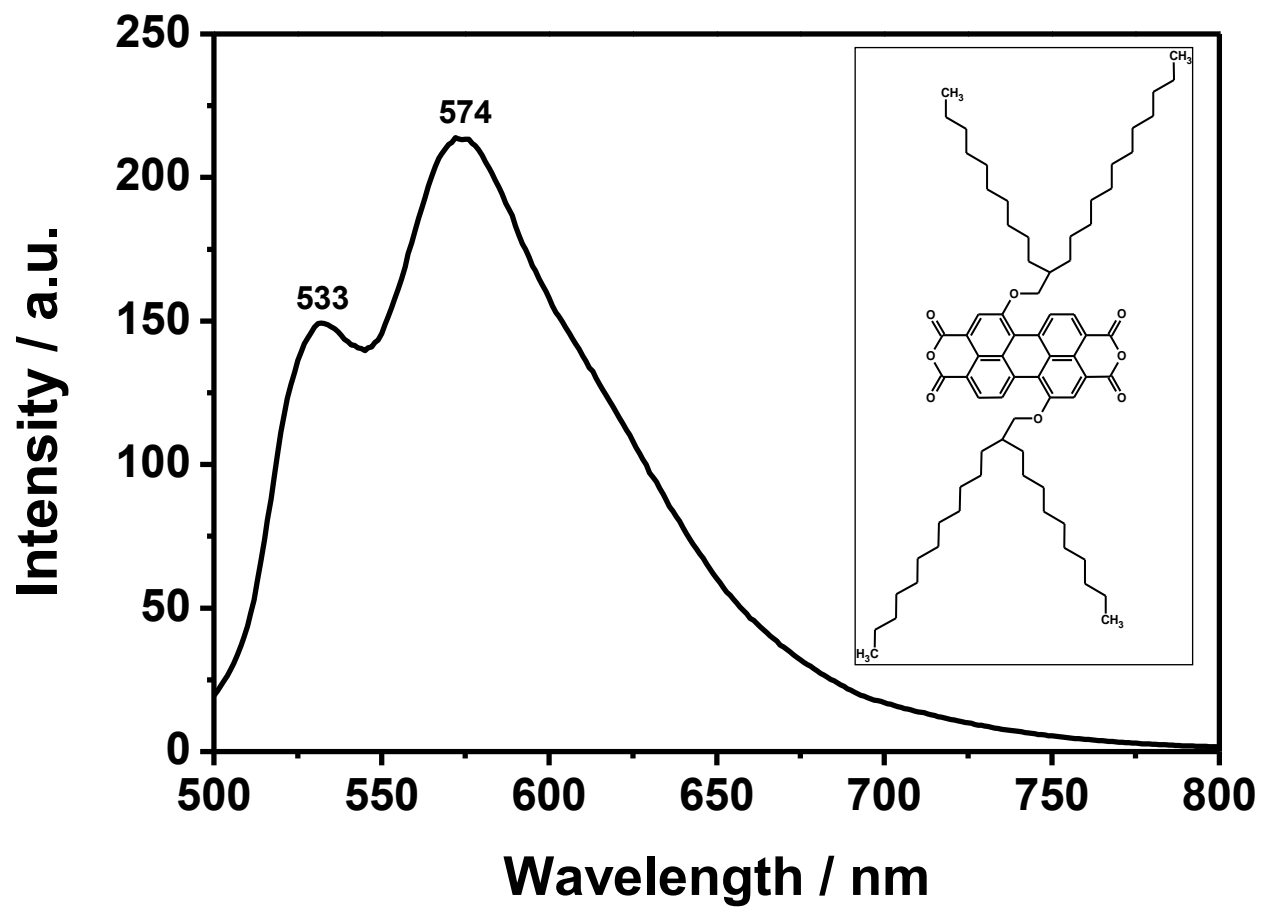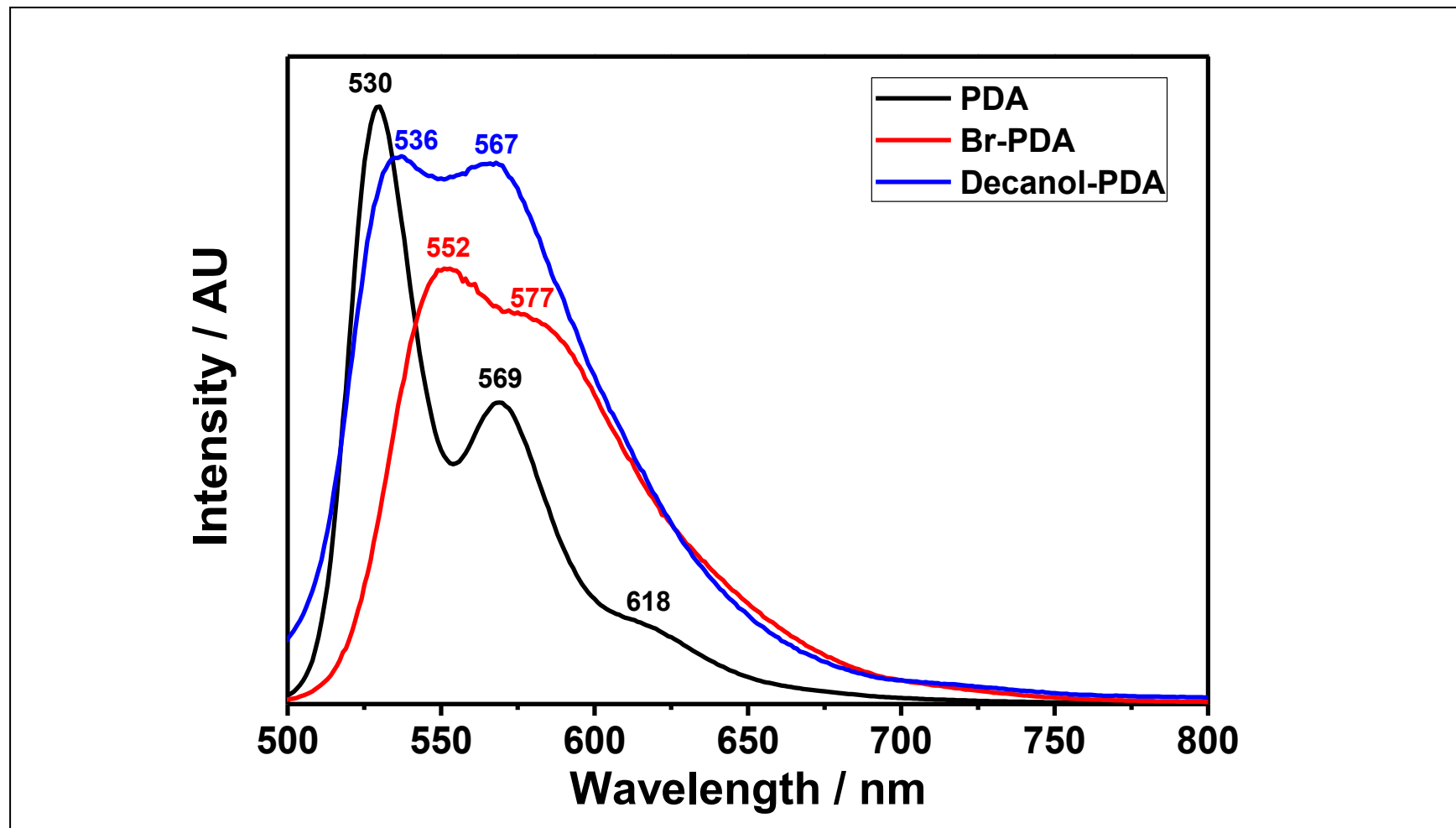
Figure 4.22: Emission spectra of PDA, Br-PDA and Decanol-PDA in DMF at λ_{exc} = 485 nm

Chapter 5

RESULTS AND DISCUSSION

5.1 Synthesis of the Designed Bay Substituted Perylene-3,4,9,10-tetracarboxylic dianhydride

1,7-di(2-decyl-1-tetradecanoyl)-perylene-3,4,9,10-tetracarboxylic dianhydride (Decanol-PDA) was successfully synthesized in two steps.

In the first step, the perylene core brominated Br-PDA was synthesized from the reaction of perylene dianhydride (PDA) with bromine in the presence of iodine and sulfuric acid. Different substituted brominated PDA derivatives can be produced from this reaction, however, special care was taken to the produce 1,7-position substituted Br-PDA as major product in main amount.

In the second step, the bromine at the bay positions of the perylene core replaced by the reaction between brominated perylene dianhydride (Br-PDA) and 2-decyl-1-tetradecanol. Subsequently, the core substituted perylene dianhydride Decanol-PDA was produced and purified by the water soxhlet.

In general, the bay substitution of perylene chromophore can be achieved easily, and provides wide varieties of core substituted perylene derivatives. 1,6-; 1,7-; and 1,6,7-core substitution are possible , where 1,6-substitution is more favorable than 1,7-substitution [2]. Therefore, in order to produce 1,7-substituted PDA as major

product, the reaction should be designed very carefully with suitable mole ratios of the reacting materials and must be accomplished accordingly. In addition, purification plays an important role to obtain the targeted 1,7-substituted perylene anhydride. The targeted 2-decyl-1-tetradecanol (1,7-substituted) core substituted perylene dianhydride (Decanol-PDA) was synthesized and purified accordingly.

5.2 Structural Characterization

The synthesized compound structures are basically confirmed by FTIR spectra; Figures (4.4, 4.5, and 4.6) shows FTIR spectra of, PDA, Br-PDA and Decanol-PDA, respectively.

The FTIR spectrum of PDA (Figure 4.4) shows the following characteristic bands: aromatic C-H stretch at 3118 cm^{-1}, anhydride C=O stretch at 1772 cm^{-1} and 1739 cm^{-1}, aromatic C=C stretch at 1594 cm^{-1} and C-O stretch at 1024 cm^{-1}.

The FTIR spectrum of Br-PDA (Figure 4.5) shows the following characteristic bands: aromatic C-H stretch at 3058 cm^{-1}, anhydride C=O stretch at 1770 cm^{-1} and 1723 cm^{-1}, aromatic C=C stretch at 1591 cm^{-1}, C-O stretch at 1036 cm^{-1} and C-Br stretch at 692 cm^{-1}.

The FTIR spectrum of Decanol-PDA (Figure 4.6) shows the following characteristic bands: aromatic C-H stretch at 3129 cm^{-1}, aliphatic C-H stretch at 2924 cm^{-1} and 2853 cm^{-1}, anhydride C=O stretch at 1765 cm^{-1} and 1734 cm^{-1}, aromatic C=C stretch at 1593 cm^{-1}, aliphatic C-H bending at 1466 cm^{-1} and C-O stretch at 1018 cm^{-1}.

5.3 Solubility

Table 5.1 shows the solubility of synthesized Br-PDA and Decanol-PDA. Both Br-PDA and Decanol-PDA are soluble in dipolar aprotic solvent (DMF), and nonpolar solvent (CHL), where Decanol-PDA has higher solubility.

On the other hand, introduction of 2-decyl-1-tetradecanol at the bay position caused to increase its solubility in nonpolar solvents (CHL) and polar protic solvents such as methanol.

Table 5.1: Solubility and Colors of the Br-PDA and Decanol-PDA in Different Solvents

Compound	Solvent	Solubility (*)	Color
Br-PDA	DMF	(− +)	Light red
	CHL	(− +)	Light red
	MeOH	(− −)	
Decanol-PDA	DMF	(+ +)	Dark green
	CHL	(+ +)	Light pink
	MeOH	(− +)	Light pink

(+ +) soluble at room temperature; (− +) partly soluble; (− −) insoluble
(*) solubility increase on heating

The thin layer chromatography (TLC) analysis for Decanol-PDA did not run even in a very polar acid eluent, owing to their polarity.

5.4 Optical Properties

5.4.1 Analysis of the UV-vis Absorption Spectra

The research on PDA on photonic and electronic properties discloses that bay substitution can significantly modify the electronic structure of perylene chromophore, and thus the electronic properties of the PDA derivatives. Furthermore, bay substitution could lead to lower the band gaps energy.

In order to use perylene derivatives in photovoltaic applications, their optical properties are very important as well electronic properties. The optical properties of the synthesized compounds are studied through absorption and emission spectra and the results are discussed.

Figure 4.7 shows the absorption spectrum of perylene-3,4,9,10-tetracarboxylic dianhydride (PDA) in dipolar aprotic solvent, DMF. The spectrum shows three main absorption peaks at 451, 484, and 517 nm, respectively, with fourth absorption peak at 588 nm. The three absorption peaks are attributed to strong π–π* electronic transitions of perylene chromophore and considered as their characteristic absorption peaks. The three absorption peaks represent 0→2, 0→1, and 0→0 transitions of perylene chromophore, respectively. The peak at 588 nm shows kind of aggregation and attributed to the strong π–π stacking interactions.

For comparison, the absorption spectrum of perylene-3,4,9,10-tetracarboxylic dianhydride (PDA) was also studied in another dipolar aprotic solvent, DMSO. As shown in the Figure 4.8, the spectrum shows three traditional perylene core absorption peaks at 454, 487, and 522 nm, respectively. In addition to this, an absorption peak at 587 nm is observed as well, that show kind of aggregation and

attributed to the strong π–π stacking interactions. The three peaks are attributed to strong π–π* electronic transitions of perylene chromophore and considered as their characteristic absorption peaks. Like in DMF, the three absorption peaks represent 0→2, 0→1 and 0→0 transitions of perylene chromophore, respectively.

Figure 4.9 shows the absorption spectrum of brominated perylene dianhydride (Br-PDA) in dipolar aprotic solvent, DMF. The spectrum shows two major absorption peaks at 489 and 516 nm, respectively. This two absorption peaks are characteristic 0→1 and 0→0 peaks that represent the strong π–π* electronic transition of perylene core. In addition, there are two weak and broad absorption peaks at 701 and 764 nm, respectively. These bands are due to the strong π-π stacking interactions between perylene cores.

Figure 4.10 shows the absorption spectrum of brominated perylene dianhydride (Br-PDA) in nonpolar solvent, CHL. The spectrum shows three characteristic absorption peaks at 455, 487 and 520 nm, respectively, which are due to π–π* transition absorptions of perylene chromophore. There is no aggregation that is observed in DMF, in the absorption spectrum for Br-PDA in CHL.

Figure 4.11 shows the absorption spectrum of core 2-decyl-1-tetradecanol substituted perylene dianhydride (Decanol-PDA) in dipolar aprotic solvent, DMF. The spectrum shows two major absorption peaks at 417 and 482 nm, respectively, that are due to π–π* electronic transitions of perylene core, in addition to them, there are two more peaks at 691 and 751 nm, respectively. This is probably due to the presence of long alkyl chains at the bay positions, and strong interactions between perylene molecules. This interaction is stronger than the π–π* electronic transition and caused a

hypsochromic shifts for the 0→1, and 0→0 characteristic peaks of perylene chromophore.

Figure 4.12 shows the absorption spectrum of core 2-decyl-1-tetradecanol substituted perylene dianhydride (Decanol-PDA) in nonpolar solvent, CHL. The spectrum shows three major characteristic absorption peaks at 480, 515 and 547 nm, respectively. The aggregation that observed from the absorption spectrum for Decanol-PDA in DMF does not observed in the absorption spectrum of Decanol-PDA in CHL.

Figure 4.13 shows the absorption spectrum of core 2-decyl-1-tetradecanol substituted perylene dianhydride (Decanol-PDA) in polar protic solvent, MeOH. The spectrum shows a broad absorption peak at around 509 nm. In addition to this, another weak and broad absorption peak at 668 nm is observed.

5.4.2 Analysis of Emission Spectra

Figure 4.14 shows the emission spectrum of perylene-3,4,9,10-tetracarboxylic dianhydride (PDA) in dipolar aprotic solvent, DMF. The spectrum shows three characteristic emission peaks of perylene core at 530, 569 and 618 nm, respectively. The three emission peaks represent $0 \rightarrow 0$, $0 \rightarrow 1$ and $0 \rightarrow 2$ electronic transitions, respectively. There is no effect of the additional absorption peak on the corresponding emission spectrum.

Figure 4.15 shows the emission spectrum of perylene-3,4,9,10-tetracarboxylic dianhydride (PDA) in another dipolar aprotic solvent, DMSO. The spectrum shows two emission peaks at 533, and 610 nm, respectively. The emission peaks are not well resolved. It has excimer-like emission.

Figure 4.16 shows the emission spectrum of brominated perylene dianhydride (Br-PDA) in dipolar aprotic solvent, DMF. The spectrum shows two emission peaks at 552 and 577 nm, respectively. Interestingly, in the same solvent, the two additional peaks found in absorption spectra of the Br-PDA have no significance on the emission spectra of the Br-PDA.

Figure 4.17 shows the emission spectrum of brominated perylene dianhydride (Br-PDA) in nonpolar solvent, CHL. The spectrum shows two emission peaks at 552 and 579 nm, respectively. However, they are not well resolved.

Figure 4.18 shows the emission spectrum of 2-decyl-1-tetradecanol substituted perylene dianhydride (Decanol-PDA) in dipolar aprotic solvent, DMF. The spectrum

shows two emission peaks at 536 and 567 nm, respectively. The peaks are not well resolved.

Figure 4.19 shows the emission spectrum of 2-decyl-1-tetradecanol substituted perylene dianhydride (Decanol-PDA) in nonpolar solvent, CHL. The spectrum shows two emission peaks at 533 and 574 nm, respectively. The excimer-like emission is observed in its emission spectrum.

Figure 4.20 shows the emission spectrum of 2-decyl-1-tetradecanol substituted perylene dianhydride (Decanol-PDA) in polar protic solvent, MeOH. The spectrum shows a broad emission peak at around 587 nm. There is a great effect of the absorption peak on its emission spectrum. Excimer-like emission spectrum is observed in the emission spectrum, as well.

Figure 4.21 shows the absorption spectrum of PDA, Br-PDA and Decanol-PDA in dipolar aprotic solvent, DMF. Their different interactions are observed. Their different properties prove the successful synthesis of Decanol-PDA. Also shows by introducing different substituents how the electronic properties are changing.

Figure 4.22 shows the emission spectrum of PDA, Br-PDA and Decanol-PDA in dipolar aprotic solvent, DMF. As it is observed, the core substituted Br-PDA and Decanol-PDA has similar emission spectrum. However, a bathochromic shift is observed in the emission spectrum of Decanol-PDA. Core substituted PDA have excimer-like emission.

Chapter 6

CONCLUSION

A novel bay substituted perylene dianhydride, Decanol-PDA was successfully synthesized in two steps. In the first step, the perylene core at 1,7-positions was brominated, to produce Br-PDA from the reaction between perylene dianhydride (PDA) and bromine. In the second step, the Br-PDA was used to synthesize the targeted bay substituted perylene dianhydride Decanol-PDA by introducing the 2-decyl-1-tetradecanol at the bay positions (1,7-positions).

Both of the products were purified, and their structures characterized by FTIR spectra. The optical properties have studied by UV-vis absorption and emission spectroscopy. The UV-vis and emission spectra were recorded at different solvents (dipolar aprotic, polar protic and nonpolar).

The Decanol-PDA show very high solubility in dipolar aprotic solvents and nonpolar solvents, this is due to the presence of the aliphatic long branched chain at the bay regions of the perylene chromophore. On the other hand, Decanol-PDA has shown moderate solubility in polar protic solvents.

The UV-vis absorption spectra of Br-PDA and Decanol-PDA in dipolar aprotic solvents show additional absorption bands at higher wavelength. These bands are suggesting the aggregations due to strong π–π stacking interactions. While, the UV-vis

absorption spectra of the two synthesized perylene derivatives in nonpolar solvent show three characteristic absorption bands, that are belonging to π–π* electronic transitions of perylene chromophore.

The emission spectra of the synthesized compounds show excimer-like emission spectra in nonpolar solvent and dipolar aprotic solvent.

REFERENCES

[1] Icil, H., Icli, S., & Sayil, Ç. (1998). Synthesis and Properties of a New Photostable Soluble Perylene Dye: N,N'-di-(L-dehydroabietyl)perylene-3,4,9,10-bis(dicarboximide). *Spectroscopy Letters.* 31(8), 1643–1647.

[2] Bagui, M., Dutta, T., Zhong, H., Li, S., Chakraborty, S., Keightley, A., & Peng, Z. (2012). Synthesis and Optical Properties of Perylene Diimide Derivatives with Triphenylene-Based Dendrons Linked at the Bay Positions Through a Conjugated Ethynyl Linkage. *Tetrahedron.* 68, 2806–2818.

[3] Kang, H., Jiang, W., & Wang, Z. (2013). Construction of Well-Defined Butadiynylene-Linked Perylene Bisimide Arrays via Cross-Coupling. *Dyes and Pigments.* 97, 244–249.

[4] Kozma, E., Kotowski, D., Catellani, M., Luzzati, S., Famulari, A., & Bertini, F. (2013). Synthesis and Characterization of New Electron Acceptor Perylene Diimide Molecules for Photovoltaic Applications. *Dyes and Pigments.* 99, 329–338.

[5] Miasojedovas, A., Kazlauskas, K., Armonaite, G., Sivamurugan, V., Valiyaveettil, S., Grazulevicius, J. V., & Jursenas, S. (2012). Concentration Effects on Emission of Bay-Substituted Perylene Diimide Derivatives in a Polymer Matrix. *Dyes and Pigments.* 92, 1285–1291.

[6] Sun, R., Xue, C., Owak, M., Peetz, R. M., & Jin, S. (2007). Facile Synthesis of Chiral Unsymmetric Perylene Tetracarboxylic Diimides Involving α-Amino Acids. *Tetrahedron Letters*. 48, 6696–6699.

[7] Xue, C., Chen, M., & Jin, S. (2008). Synthesis and Characterization of the First Soluble Nonracemic Chiral Main-Chain Perylene Tetracarboxylic Diimide Polymers. *Polymer.* 49, 5314–5321.

[8] Yu, Y., Li, Y., Qin, Z., Jiang, R., Liu, H. & Li, Y. (2013). Designed Synthesis and Supramolecular Architectures of Furan-Substituted Perylene Diimide. *Journal of Colloid and Interface Science*. 399, 13–18.

[9] Koyuncu, S., Kus, M., Demic, S., Kaya, I., Ozdemir, E., & Icli, S. (2008). Electrochemical and Optical Properties of Novel Donor-Acceptor Thiophene-Perylene-Thiophene Polymers. *Journal of Polymer Science: Part A: Polymer Chemistry*. 46, 1974–1989.

[10] Uzun, D., Ozser, M. E., Yuney, K., Icil, H., & Demuth, M. (2003). Synthesis and Photophysical Properties of N,N′-bis(4-cyanophenyl)-3,4,9,10-perylenebis(dicarboximide) and N,N′-bis(4-cyanophenyl)-1,4,5,8-naphthalenediimide. *Journal of Photochemistry and Photobiology A: Chemistry*.156, 45–54.

[11] Pasaogullari, N., Icil, H., & Demuth, M. (2006). Symmetrical and Unsymmetrical Perylene Diimides: Their Synthesis, Photophysical and Electrochemical Properties. *Dyes and Pigments*. 69, 118–127.

[12] Dinçalp, H., Aşkar, Z., Zafer, C., & Içli, S. (2011). Effect of Side Chain Substituents on the Electron Injection Abilities of Unsymmetrical Perylene Diimide Dyes. *Dyes and Pigments*. 91, 182–191.

[13] Oner, I., Varlikli, C., & Icli, S. (2011). The Use of a Perylenediimide Derivative as a Dopant in Hole Transport Layer of an Organic Light Emitting Device. *Applied Surface Science*. 257, 6089–6094.

[14] Kozma, E., & Catellani, M. (2013). Perylene Diimides Based Materials for Organic Solar Cells. *Dyes and Pigments*. 98, 160–179.

[15] Bodapati, J. B., & Icil, H. (2008). Highly Soluble Perylene Diimide and Oligomeric Diimide Dyes Combining Perylene and Hexa(ethylene glycol) Units: Synthesis, Characterization, Optical and Electrochemical Properties. *Dyes and Pigments*. 79, 224–235.

[16] Huo, L., Zhou, Y., & Li, Y. (2008). Synthesis and Absorption Spectra of n-Type Conjugated Polymers Based on Perylene Diimide. *Macromol. Rapid Commun.* 29, 1444–1448.

[17] Icil, H., & Icli, S. (1997). Synthesis and Properties of a New Photostable Polymer: Perylene-3,4,9,10-tetracarboxylic Acid–bis-(N,N'-dodecylpolyimide*). Journal of Polymer Science Part A: Polymer Chemistry*. 35, 2137–2142.

[18] Jancy, B., & Asha, S. K. (2009). Synthesis and Self-Organization Properties of Copolyurethanes Based on Perylenediimide and Naphthalenediimide Units. *Journal of Polymer Science Part A: Polymer Chemistry*. 47(4), 1224–1235.

[19] Liang, Z., Cormier, R. A., Nardes, A. M., & Gregg, B. A. (2011). Developing Perylene Diimide Based Acceptor Polymers for Organic Photovoltaics. *Synthetic Metals.* 161, 1014–1021.

[20] Vivo, P., Dubey, R., Lehtonen, E., Kivistö, H., Vuorinen, T., & Lemmetyinen, H. (2013). Dipyrrolidinyl-Substituted Perylene Diimide as Additive for Poly(3-Hexylthiophene): [6,6]-Phenyl C61 Butyric Acid Methylester Bulk-Heterojunction Blends. *Thin Solid Films.*548, 398–405.

[21] Xu, S., Jin, Y., Yang, M., Bai, F., & Cao, F. (2006). Highly Soluble Diphenylfluorene-based Cardo Copolyimides Containing Perylene Units. *Polym. Adv. Technol*. 17, 556–561.

[22] Yao, D., & Sundararajan, P. R. (2006). Effect of Conformational Adaptation of 4,4'-(hexafluoro-isopropylidene) Diphthalic Anhydride (6FDA) on the Structural Features of a Perylene-containing Copolyimide. *European Polymer Journal*. 42, 302–310.

[23] Yuney, K., & Icil, H. (2007). Synthesis, Photochemical, and Electrochemical Properties of Naphthalene-1,4,5,8-tetracarboxylic acidbis-(N,N'-bis-(2,2,4(2,4,4)-trimethylhexylpolyimide)) and Poly(N,N'-bis-(2,2,4(2,4,4)-trimethyl-6-

aminohexyl)3,4,9,10-perylenetetracarboxdiimide. *European Polymer Journal*. 43, 2308–2320.

[24] Cui, Y., Yao, D., Chen, Y., & Wang, Z. (2012). Synthesis and Properties of Novel Functional Polymers from Tetrachlorinated Perylene Bisimide. *Journal of Polymer Science Part A: Polymer Chemistry*. 50, 3485–3492.

[25] Rusu, R. -D., Damaceanu, M. -D., & Bruma, M. (2010). Aromatic Copolyimides Containing Perylene Units. *Macromol. Symp*. 296, 399–406.

[26] Bodapati. J B (2011) PhD Thesis, Eastern Mediterranean University.

[27] Muth, M. -A., Carrasco-Orozco, M., & Thelakkat, M. (2011). Liquid-Crystalline Perylene Diester Polymers with Tunable Charge-Carrier Mobility. *Adv. Funct. Mater.* 21, 4510–4518.

[28] Gawrys, P., Boudinet, D., Zagorska, M., Djurado, D., Verilhac, J. -M., Horowitz, G., Pécaud, J., Pouget, S., & Pron, A. (2009). Solution Processible Naphthalene and Perylene Bisimides: Synthesis, Electrochemical Characterization and Application to Organic Field Effect Transistors (OFETs) Fabrication. *Synthetic Metals.* 159, 1478–1485.

[29] Nazeeruddin, M. K., Baranoff, E., & Grätzel, M. (2011). Dye-sensitized Solar Cells: A Brief Overview. *Solar Energy.* 85, 1172–1178.

[30] Miles, R. W., Hynes, K. M., & Forbes, I. (2005). Photovoltaic Solar Cells: An Overview of State-of-the-art Cell Development and Environmental Issues. *Progress in Crystal Growth and Characterization of Materials*. 51, 1–42.

[31] Sharma, G. D., Roy, M. S., Mikroyannidis, J. A., & Thomas, K. R. J. (2012). Synthesis and Characterization of a New Perylene Bisimide (PBI) Derivative and its Application as Electron Acceptor for Bulk Heterojunction Polymer Solar Cells. *Organic Electronics*. 13, 3118–3129.

[32] Hoppe, H., & Sariciftci, N. S. (2004). Organic Solar Cells: An Overview. *J. Mater. Res.* 19(7), 1924–1945.

[33] Nakamura, J. –I., Yokoe, C., Murata, K., & Takahashi., K. (2004). Efficient Organic Solar Cells by Penetration of Conjugated Polymers into Perylene Pigments. *Journal of Applied Physics.* 96(11), 6878–6883.

[34] Neuteboom, E. E., Meskers, S. C. J., Meijer, E. W., & Janssen, R. A. J. (2004). Photoluminescence of Self-organized Perylene Bisimide Polymers. *Macromol. Chem. Phys*. 205, 217–222.

[35] Pron, A., & Leclerc, M. (2013). Imide/Amide Based π-conjugated Polymers for Organic Electronics. *Progress in Polymer Science*. 38, 1815–1831.

[36] Liaw, D. -J., Wang, K. -L., Huang, Y. C., Lee, K. -R., Lai, J. -Y., & Ha, C. -S. (2012). Advanced Polyimide Materials: Syntheses, Physical Properties and Applications. *Progress in Polymer Science*. 37, 907–974.

[37] Guo, X., Baumgarten, M., & Müllen, K. (2013). Designing π-conjugated Polymers for Organic Electronics. *Progress in Polymer Science.* 38, 1832–1908.

[38] Ego, C., Marsitzky, D., Becker, S., Zhang, J., Grimsdale, A. C., Müllen, K., MacKenzie, J. D., Silva, C., & Friend, R. H. (2003). Attaching Perylene Dyes to Polyfluorene: Three Simple, Efficient Methods for Facile Color Tuning of Light-Emitting Polymers. *J. Am. Chem. Soc.* 125, 437–443.

[39] Shinar, J., Shinar, R. (2008). Organic Light-Emitting Devices (OLEDs) and OLED-based Chemical and Biological Sensors: An Overview. *J. Phys. D: Appl. Phys*. 41, 133001 (26pp).

[40] Ko, H. C., Lim, D. K., Kim, S. -H., Choi, W., & Lee, H. (2004). Light-Emitting Electrochemical Cells Based on Polyimide Containing Perylene and Tri(ethylene Oxide) Moieties. *Synthetic Metals*. 144, 177–181.

[41] Ohta, T., Nagano, T., Ochi, K., Kubozono, Y., & Fujiwara, A. (2006). Field-Effect Transistors With Thin Films of Perylene on SiO_2 and Polyimide Gate Insulators. *Appl. Phys. Lett*. 88, 103506(1–3).

[42] Scaiano, J. C. (1989). (Ed.). Handbook of Organic Photochemistry, CRC press.

[43] Turro, N. J. (1965) Molecular Photochemistry, Benjamin, London, 44.